Robotica (2018) volume 36, pp. 1641–1663. © Cambridge University Press 2018
doi:10.1017/S0263574718000619

Kinematic topology and constraints of multi-loop linkages

Andreas Müller*

Institute of Robotics, Johannes Kepler University, Linz, Austria

(Accepted June 30, 2018. First published online: August 2, 2018)

SUMMARY

Modeling the instantaneous kinematics of lower pair linkages using joint screws and the finite kinematics with Lie group concepts is well established on a solid theoretical foundation. This allows for modeling the forward kinematics of mechanisms as well the loop closure constraints of kinematic loops. Yet there is no established approach to the modeling of complex mechanisms possessing multiple kinematic loops. For such mechanisms, it is crucial to incorporate the kinematic topology within the modeling in a consistent and systematic way. To this end, in this paper a kinematic model graph is introduced that gives rise to an ordering of the joints within a mechanism and thus allows to systematically apply established kinematics formulations. It naturally gives rise to topologically independent loops and thus to loop closure constraints. Geometric constraints as well as velocity and acceleration constraints are formulated in terms of joint screws. An extension to higher order loop constraints is presented. It is briefly discussed how the topology representation can be used to amend structural mobility criteria.

KEYWORDS: Topology; Kinematics; Constraints; Mobility; Jacobian; Screws; Lie Groups.

1. Introduction

The modeling of mechanism kinematics is a core topic in mechanism theory and indispensable for the analysis, design and control of robotic manipulators. For mobility and singularity analysis, in particular, for most methods the key element is the system of closure constraints. The first-order (velocity) constraints for lower pair linkages in particular are given in terms of the instantaneous joint screw coordinates.[40] Moreover, screw theory is the established geometric foundation for the analysis of the instantaneous kinematics of linkages.[6] When dealing with multi-loop linkages, however, the models are often introduced ad hoc rather than following a systematic approach that takes into account the mechanism topology. In order to systematically treat multi-loop linkages, a graph-based approach has been introduced by Davis[7–9] and, with small variations, was applied to the first-order mobility analysis of linkages for instance in ref. [44,53]. Unfortunately, these graph-based descriptions are not commonly used. One consequence of the lack of a universal representation of the kinematic topology is that in various publications constraints are introduced for topologically dependent loops.

Screw theory combined with Lie group theory provides the mathematical framework also for describing the finite motions of mechanisms,[3,30–32,40,46] and hence for the finite mobility and singularity analysis[16,26,27,34] involving geometric and higher order constraints in terms of joint screw coordinates. These formulations were derived for single-loop linkages and then applied to multi-loop linkages in an ad hoc manner. A systematic formulation for the higher order constraints of multi-loop linkages is still due.

The key to the modeling of multi-loop mechanisms is a systematic representation of the kinematic topology. This has been an integral part of multibody system (MBS) dynamics from its very beginning,[51,52] and is clearly relevant for mechanism modeling. The modeling of complex MBS relies on a graph representation of the kinematics that allows for algorithmic manipulation. Furthermore, mechanisms with structural symmetries has become a topic in mechanism theory and robotics since the

* Corresponding author. E-mail: a.mueller@jku.at

https://doi.org/10.1017/S0263574718000619 Published online by Cambridge University Press

advent of parallel manipulators (PKM).[22] In this context, tailored approaches to represent the kinematic topology were introduced such as the structural graph.[13] For providing a tool for representing PKM topologies, these approaches are not applicable to general mechanisms, however.

In this paper, a graph representation of the kinematic topology is proposed and used to formulate loop closure constraints. A short overview of graph representations of mechanisms is given in Section 2. The notion of a topological graph is recalled in Section 3, and a kinematic model graph is introduced. The latter gives rise to a system of topologically independent fundamental cycles (FCs) and an ordering of joints and bodies within the mechanism. A formulation of loop closure constraints is introduced in Section 4, using the graph representation of kinematic topology noting that edges of the kinematic graph represent screw joints. The geometric constraint are formulated first. Then the corresponding velocity and acceleration constraints are derived. It is briefly outlined how higher order constraints (jerk, jounce, etc.) can be derived. All higher order constraints are given in terms of Lie brackets (screw products) of instantaneous joint screw coordinates. In Section 5, a formulation for the forward kinematics of mechanisms is presented. It is briefly described in Section 6 how the proposed modeling approach can be used for modeling mechanism comprising identical submodules. A short discussion on the significance of the topology representation for structural mobility criteria is given in Section 7. The basic relations for screw/Lie group modeling are summarized in the appendix. Throughout the paper, the 3URU fully parallel manipulator[55] and the metamorphic five finger hand proposed in ref. [47] are used as examples.

2. Overview of Existing Graph Representations for Kinematic Chains

2.1. Structural and topological graph

Structural/topological graphs are important for the structural synthesis of mechanisms, i.e., the general arrangement of the mechanical structure, the type and number of joints, and the way they are connected.[22] The *structural graph* is an established schematic representation[13] showing the basic setup. Edges and vertices represent bodies and joints, respectively. Body labels become the indices of the vertices. Edges are not necessarily indexed but the type of joint is indicated with **U** (universal), **R** (revolute), **S** (spherical). Figure 2a shows the structural graph of the 3URU PKM in Fig. 1 that was presented in ref [55]. For actuated mechanisms, it is also common to underline the actuated joints. Clearly, this is a rather coarse information since for the 3URU PKM only the first revolute joint is actuated.

In order to refer to individual bodies and joints they can be labeled uniquely. Their arrangement is then represented by the *topological graph* Γ (see Section 3.1 for precise definition). This provides a systematic representation facilitating kinematic and dynamic algorithms.[14,51] Figure 2b shows the topological graph for the 3URU manipulator.

2.2. Coupling graph

Within the network approach to the kinetostatic modeling of kinematic chains, Davis[8,9] introduced a *coupling graph*. This is obtained from the topological graph by introducing directions. The direction of an edge allows to interpret the relative motion generated by the corresponding kinematic coupling between two bodies.

2.3. Motion graph and constraint graph

The motion of a δ-DOF coupling (represented by an edge in the coupling graph) can be expressed in terms of δ local coordinates (at least locally). In other words, it can be modeled as concatenation of successive 1-DOF motions. Davis[8,9] calls the (directed) graph, obtained by replacing an edge of the coupling graph that represents a δ-DOF coupling by δ edges in series, the *motion graph*. The latter is closely related to the kinematic model graph introduced in Section 3.2. Figure 8a shows this for the 3URU example.

The motion graph represents the motion possibilities in that each edge corresponds to one DOF of the relative motion of adjacent bodies. Its counterpart is the *constraint graph*. This is the graph obtained from the topological graph by replacing each edge representing a δ-DOF by as many parallel edges as the joint imposes constraints, i.e., generically $6-\delta$ edges. The constraint graph for the 3URU example is shown in Fig. 2c.

https://doi.org/10.1017/S0263574718000619 Published online by Cambridge University Press

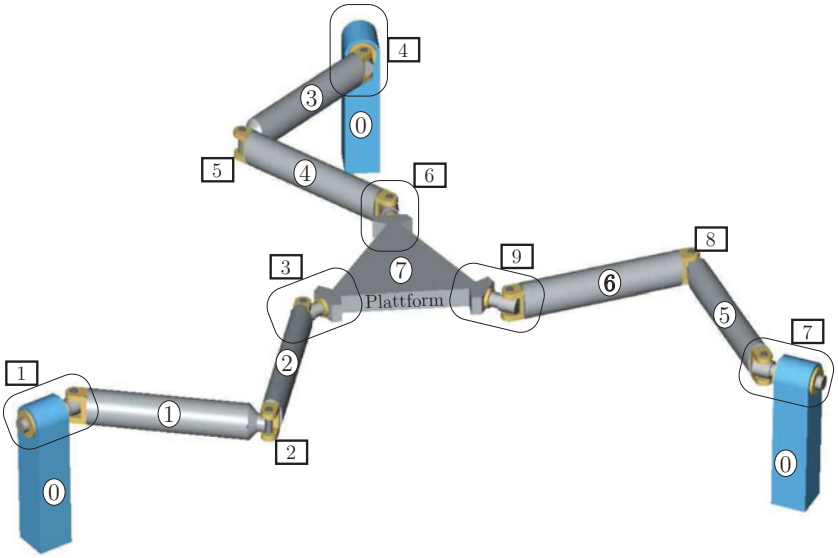


Fig. 1. 3URU – Parallel manipulator after Zlatanov *et al.*[55] The universal joints are encircled.

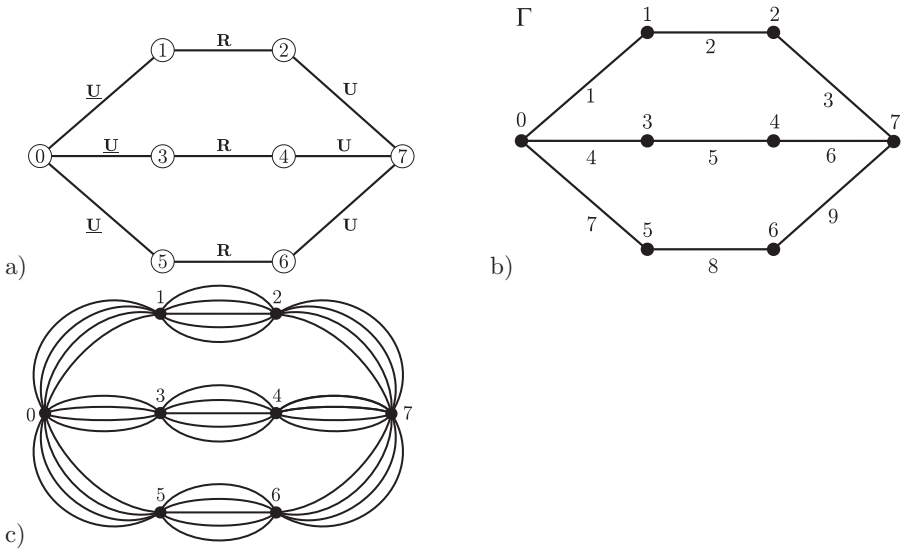


Fig. 2. (a) Structural graph[13] for the 3URU manipulator, (b) its topological graph Γ, (c) constraint graph.

Remark 1. An important question is whether, within a mechanism, there are redundant constraints for generic geometries. The constraint graph provides a basis for answering this. To this end, combinatorial algorithms like the so-called pebble game are used.[43] Such algorithms further allow for decomposing a constraint graph into Assur graphs. Assur groups form a topic that is receiving increasing attention as it allows for constructing kinematic chains without imposing redundant constraints, at least for generic geometries. Graphs associated with Assur groups are called Assur graphs. Davis referred to them as "virtual coupling" as they may simply be considered as a (complex) coupling of two or more bodies.

2.4. Body-hinge graphs

Body-hinge graphs are widely used to model molecular systems, where hinges represent hydrogen bonds,[49] and molecules are regarded as articulated kinematic chains. In the mathematical field of rigidity theory, combinatorial algorithms were developed to check for rigid substructures of these graphs. Body-hinge graphs are special topological graphs for kinematic chains comprising only revolute joints. Usually there is no more than one edge (revolute joint) between two vertices (bodies).

https://doi.org/10.1017/S0263574718000619 Published online by Cambridge University Press

2.5. Body-Bar graphs

Body-bar graphs can be seen as a special version of constraint graphs.[18] Edges are interpreted as bars, and each edge represents one distance constraint imposed between two bodies (vertices). This allows for modeling various couplings. The replacement of various lower pair joints was reported in ref. [48]. The equivalence is, however, only valid instantaneously in general. A prismatic joint, for example, is represented by a rotation about an axis at infinity.

2.6. Bar-joint graphs

Bar-Joint graphs stem from rigidity theory.[19,20,50] Vertices represent points in $\mathbb{R}^n$ whose positions are described by Cartesian coordinates. Bar-Joint graphs are thus well-suited to represent the kinematic relations of a set of points subjected to distance constraints. The latter are interpreted as bars, while the vertices/points are treated as "joints." More precisely the "joints" are regarded as spherical joints in $\mathbb{R}^3$ and as revolute joints in $\mathbb{R}^2$. Care must be exercised in $\mathbb{R}^3$, however, since, according to this interpretation the bars would be free to rotate about their longitudinal axes. This mobility is ignored in all algorithms for the mobility/rigidity determination of bar-joint networks.[43,50] No physical extension or inertia properties are associated with the bars. Bar-joint graphs are used to model molecular systems where vertices represent atoms subjected to distance constraints. An extension to MBSs has been presented in ref. [45] where rigid subgraphs of points are assigned dynamic properties.

Bar-joint graphs allow for the presence of "multiple joints," i.e., vertices with more than two edges.[10,54] The conversion of a bar-joint graph with multiple joints to a body-bar graph representation is not unique. A multiple joint connecting b bars corresponds $b-1$ joints in the body-bar graph. The assignment of these $b-1$ joints is not unique as shown in ref. [29]. A recent approach to account for multiple joints in structural mobility formulae can be found in ref [38].

Beside in rigidity theory, bar-joint graphs are mainly employed in mechanism theory for the purpose of graph-based synthesis of mostly planar linkages with hinges.[10] Bar-joint graphs are also used for kinematic analysis of mechanisms using a distance-based formulation.[37] For general kinematic modeling, bar-joint, body-bar, as well as body-hinge graphs are not widely used.

3. Proposed Representation of the Kinematic Topology

3.1. Topological graph

The basic structural information of a mechanism is the number of links and joints, and the types of joints. The kinematic topology of a mechanism refers to the adjacency of bodies and joints. This incidence relation is represented by the topological graph[25] denoted by $\Gamma = (B, J, \delta)$. The latter is an edge- and vertex-labeled multi-graph with vertex set B, edge set J, and edge weight function δ. Vertices represent rigid bodies and edges represent joints (or general kinematic couplings). One body is regarded as the reference body, usually the ground, which is labeled with 0, and $B_0 \in B$ is its corresponding vertex. The newly created vertices (bodies) are labeled with $B_\alpha \in B$, $\alpha = 1, \ldots, |B| - 1$. Edges (joints) are labeled with $J_i \in J$, $i = 1, \ldots, |J|$. This vertex labeling is advantageous for the kinematic modeling.

The topological graph Γ is undirected. It is possibly a multi-graph, i.e. there can be more than one edge (joint) between two vertices (bodies). Γ is an edge-weighted graph, where the "weight" of an edge represents the essential information about the joint it represents. This weight is usually the DOF $\delta_i = \delta(J_i)$ of joint i. It could also be the type of joint as in case of the structural graph (Fig. 2a). For the actual kinematic modeling, more specific information is required, however. This requires a kinematic model and leads to the associated graph in the next section.

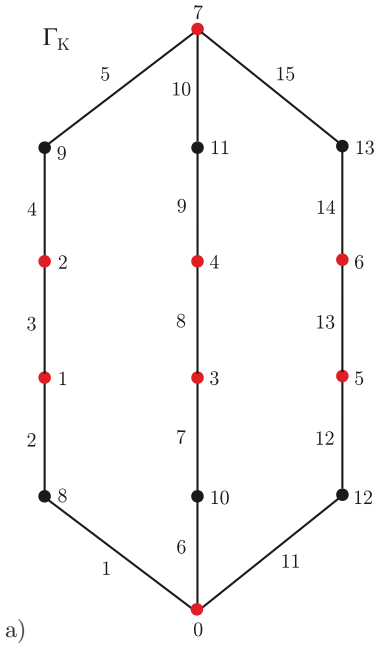
Example 1: Figure 2b shows the topological graph of the 3URU manipulator example. It comprises $|B| = 8$ bodies (including the ground B_0) and $|J| = 9$ joints.

3.2. Kinematic model graph

The kinematics of the mechanism is described in terms of joint variables. The following assumption is crucial for the kinematics formulation introduced later in the paper.

Assumption 3.1. All joints can be modeled by combination of screw joints, i.e., of revolute, prismatic or proper screw joints. The mechanism is thus considered as a linkage.

https://doi.org/10.1017/S0263574718000619 Published online by Cambridge University Press



a)

b)

Edge $J_i \in \Gamma$ (Joint)	Edge $e_i \in \Gamma_K$ (Joint Variables)
1	1 2
2	3
3	4 5
4	6 7
5	8
6	9 10
7	11 12
8	13
9	14 15

Fig. 3. (a) Kinematic graph Γ_K for the 3URU. Red vertices represent actual bodies and are adopted from the topological graph Γ in Fig. 2b. (b) Relation of joints, i.e., edges of the topological graph in Fig. 2b, and edges of the kinematic graph Γ_K.

A joint with DOF δ_i is thus modeled by combination of δ_i 1-DOF screw joints. This is not reflected in the topological graph, which motivates the following.

Definition 1. The *kinematic model graph* (or simply *kinematic graph*) is the undirected (multi-) graph, denoted by $\Gamma_K(V, E)$, obtained from the topological graph by replacing an edge $J_i = \left(B_\beta, B_\alpha\right) \in \Gamma$, which represents a joint with DOF δ_i, by a sequence of δ_i edges and $\delta_i - 1$ vertices. The total number of edges is denoted with $n := |E|$.

Here E is the set of edges, and V is the set of vertices. An edge represents exactly one DOF of the relative motion of adjacent bodies. Thus, n is the total number of joint variables. The additionally introduced vertices may be regarded as representing auxiliary bodies. As for the topological graph, vertices are labeled with lower case greek letters, $v_\alpha \in V, \alpha = 0, \ldots |V| - 1$. The vertex labeling is arbitrary, in principle. But in order to easily associate the kinematic graph with the actual mechanism, the labeling of those vertices that represent bodies of the mechanism is carried over from the topological graph Γ (as in ref. [9]). In particular, $v_0 \in \Gamma_K$ represents the ground. The remaining vertices of Γ_K are arbitrarily labeled with $\alpha = |B|, \ldots, |V| - 1$.

Edges are unordered pairs of vertices, and are labeled with lower case Latin letters, $e_i \in E, i = 1, \ldots, n$, where $e_i = \left(v_\beta, v_\alpha\right)$ is the edge connecting vertices v_β and v_α. Edge labels are assigned arbitrarily. For a single loop linkage, the links and joints are usually numbered consecutively with $i = 1, \ldots, n$.

Example 1 (cont.): Figure 3a shows the kinematic graph for the 3URU manipulator in Fig. 1. Since the six universal joints are, respectively, parameterized by two joint angles (i.e., replaced by two revolute joints), it contains $|V| = 14$ vertices and $n = 15$ edges. The edge $J_1 \in J$ (universal joint 1), for instance, is replace by the two edges $e_1, e_2 \in E$ (each representing a revolute joint) together with the vertex $v_1 \in V$ (that may be regarded as representing the cross/spider). The correspondence of joints and vertices of Γ_K is given in Fig. 3b. Vertices $B_\alpha \in B$ (bodies of the linkage) in the topological graph become vertices $v_\alpha \in V$ in the kinematic graph. In Fig. 3a, $v_7 \in V$ corresponds to the platform body.

Example 2: The metamorphic five finger robotic hand in Fig. 4 was presented in ref. [47]. Its palm is a spherical five-bar linkage that allows for reconfiguration of the hand. Figure 5 shows its kinematic

https://doi.org/10.1017/S0263574718000619 Published online by Cambridge University Press

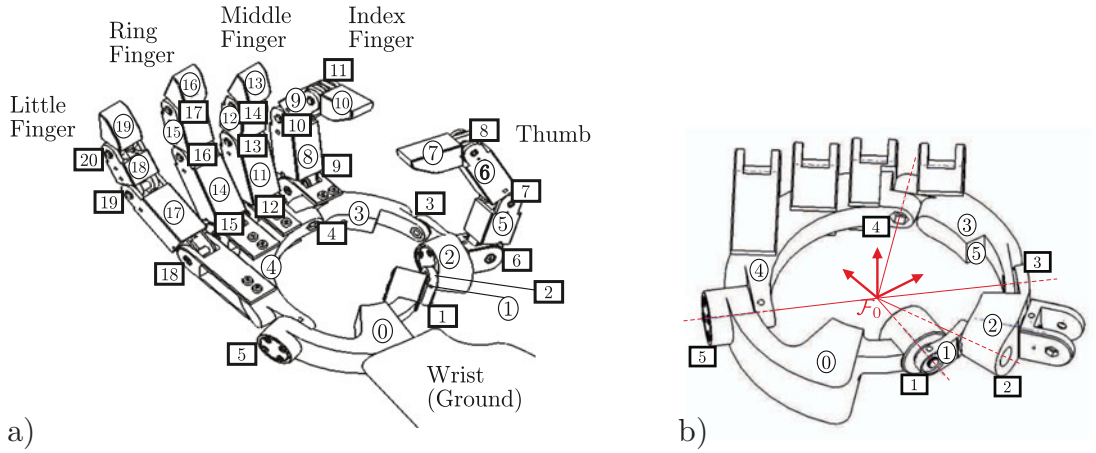


Fig. 4. (a) Drawing of the metamorphic five-finger hand. (b) Detailed drawing of the palm (spherical five-bar linkage). Figures by courtesy of Guowu Wei and Jian Dai.

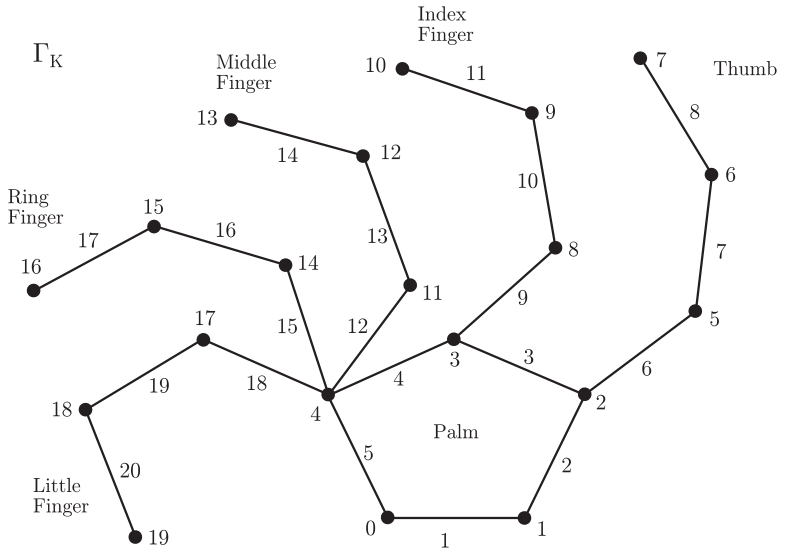


Fig. 5. Kinematic graph Γ_K for the metamorphic hand.

graph. Since this linkage comprises only 1-DOF joints the topological and kinematic graph are identical.

Remark 2. Some authors use an index notation that shall allow to associate the original numbering of joints in the topological graph to the edge labels in the kinematic graph. For example, i_j is occasionally used to denote the jth edge in Γ_K in the replacement of edge (joint) i in the topological graph Γ.

Remark 3. The transition from the topological graph to the kinematic model graph involves a kinematic modeling step. The kinematic model may not be unique because it stems from the substitution of multi-DOF joints by several 1-DOF joints, i.e., introduction of a local chart. For a given kinematic model, the kinematic graph is unique, however.
It is sometimes assumed beforehand that MBS and mechanisms are modeled in terms of 1-DOF joints.[25,26,51] In this case, the topological graph is identical to the kinematic graph.

3.3. Spanning tree and kinematic loops

A *spanning tree* can be introduced on Γ_K. A spanning tree is an acyclic subgraph containing all vertices such there is a path between any two vertices. The subgraph comprising all edges that are not in $\mathcal{G}_0$ constitutes the *co-tree* $\mathcal{H}$. To each co-tree edge corresponds exactly one FC. A FC in Γ_K is a

https://doi.org/10.1017/S0263574718000619 Published online by Cambridge University Press

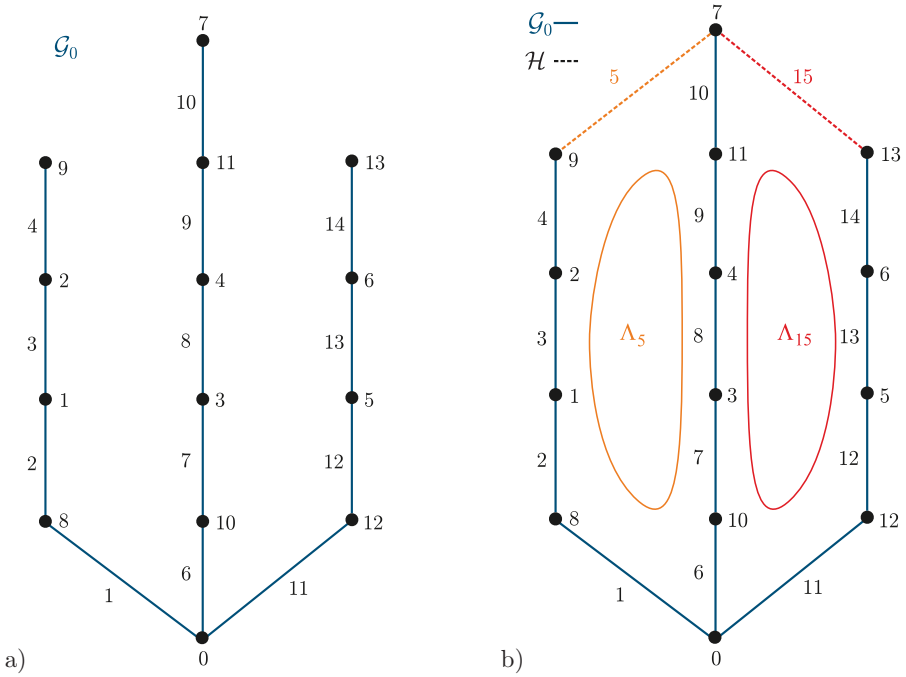


Fig. 6. (a) Spanning tree $\mathcal{G}_0$ for the kinematic graph in Fig. 3. (b) Co-tree and corresponding FCs.

closed path without repeated edges or vertices that contains exactly one co-tree edge. That is, adding any co-tree edge creates a cycle – a FC. The FC containing the co-tree edge $e_l \in \mathcal{H}$ is denoted by Λ_l. The spanning tree is not unique. A special choice, denoted by $\mathcal{G}_0$, is the spanning tree where the ground vertex v_0 is the root vertex. This will be used w.l.o.g. throughout the paper.

A graph that consists of one component (there is path between any two vertices) possesses $\gamma = |E| - |V| + 1$ FCs, respectively, co-tree edges. The importance of FCs is that they are topologically independent loops, so that only for these FCs kinematic loop constraints need to be introduced. Since $\mathcal{G}_0$, and thus $\mathcal{H}$, is generally not unique, different loop constraints can be introduced for the same mechanism. The number γ of FCs is indeed the same for Γ and Γ_K, since the construction of Γ_K from Γ does not introduce cycles. FCs are subgraphs, but are commonly indicated by a closed line next to its edges.

Example 1 (cont.): Figure 6a shows a spanning tree $\mathcal{G}_0$ for the kinematic graph of the 3URU manipulator. The corresponding co-tree and FCs are shown in Fig. 6b.

Example 2 (cont.): A spanning tree and corresponding co-tree for the metamorphic hand are shown in Fig. 7. While for the fully parallel 3URU manipulator, it is most obvious to introduce the spanning tree such that its branches correspond to the kinematically identical chains from base to platform, the spanning tree for the hand is rather arbitrary.

3.4. Global order and predecessors

The spanning tree $\mathcal{G}_0$ gives rise to a partial ordering on Γ_K, and thus allows to define a unique predecessor for any vertex and edge, which is necessary for kinematic modeling.

The edge e_j is the *direct predecessor* of e_i iff e_j comes directly after e_i within the path in $\mathcal{G}_0$ from e_i to the ground vertex. This is denoted by $e_j = e_i - 1$, or $j = i - 1$ for short. The notation $i - 2 := (i - 1) - 1$ is used to denoted the pre-predecessor of i, and $i - k$ denotes the kth predecessor of e_i. The edge e_j is *a predecessor* of e_i iff e_j is contained in the path within $\mathcal{G}_0$ from e_i to the ground vertex. This is indicated by $e_j < e_i$, or simply by $j < i$.

In $\mathcal{G}_0$ there is a unique path from any vertex v_α to the ground vertex v_0. Vertex v_β is the direct predecessor of v_α iff it comes immediately after v_α in the path from from v_α to v_0 within $\mathcal{G}_0$. Denote with $r(\alpha)$ the *root-edge*, i.e., the last edge in the path that connects to the ground vertex.

Further denote with $e(\alpha)$ the index of that edge connecting vertex v_α to its predecessor.

https://doi.org/10.1017/S0263574718000619 Published online by Cambridge University Press

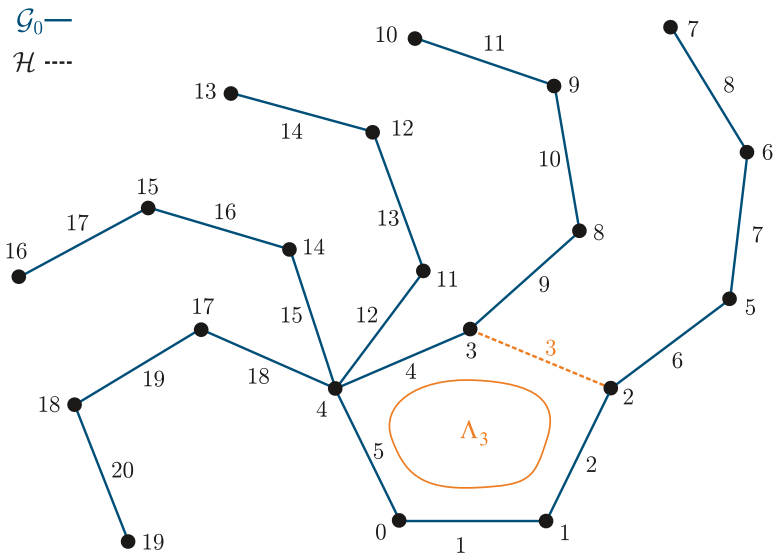


Fig. 7. Spanning tree $\mathcal{G}_0$ and co-tree $\mathcal{H}$ for the metamorphic hand.

Example 1 (cont.): The spanning tree in Fig. 6a induces the direct predecessor relations for the 3URU model. For instance, $e_1 = e_2 - 1$, $e_2 = e_3 - 1$, $e_9 = e_{10} - 1$, $e_0 = e_1 - 1 = e_6 - 1 = e_{11} - 1$. Also, $e_6 < e_8$ and $e_{11} < e_{14}$, but $e_6 \not< e_{14}$ and $e_{11} \not< e_8$, for instance. The edges that connect vertices to their predecessors are, for example, $e(1) = 2$, $e(7) = 10$. The root joint connecting the kinematic chain of bodies 3 and 7 is $r(3) = r(7) = 6$, for instance, since they are in the same kinematic chain to the ground.

3.5. Joint orientations

An edge $v_i \in \Gamma_K$ represents a 1-DOF relative (screw) motion. It remains to indicate in which direction this relative motion is measured. Moreover, the joint kinematics will be described by joint variables together with joint screw coordinates assigned to the vertices. Since these variables parameterize the relative motion of adjacent bodies, they induce an orientation of the corresponding edge (also called the polarity[11]). This is represented by the *oriented kinematic graph* denoted with $\overrightarrow{\Gamma}_K = (V, \overrightarrow{E})$, where $\overrightarrow{E}$ consists of directed edges $\vec{e}_i$. A directed edge (also called *arc*) is an ordered pair $\langle v_\beta, v_\alpha \rangle \in \overrightarrow{E}$, where v_β is referred to as the source and v_α as the target of the edge. Notice that $\langle v_\alpha, v_\beta \rangle \notin \overrightarrow{E}$.

The directed edge $\vec{e}_i = \langle v_\beta, v_\alpha \rangle \in \overrightarrow{\Gamma}_K$ indicates that the corresponding joint variable (together with the joint screw coordinates) describes the motion of (auxiliary) body α w.r.t. body β. The directions are necessary for the subsequent kinematic modeling, but can be introduced arbitrarily.

Denote with $\overrightarrow{\mathcal{G}}_0$ the *root-oriented spanning tree*, which is the unique orientation of $\mathcal{G}_0$ such that there is a (unique) directed path from v_0 to any vertex. That is, the edges are directed away from vertex v_0. Thus $\overrightarrow{\mathcal{G}}_0$ is regularly directed (other authors define regular directions such that all edges are oriented towards v_0, e.g., ref. [51]).

The directed tree $\overrightarrow{\mathcal{G}}_0$ provides a reference for measuring joint orientations. To this end, the direction of an edge of the directed kinematic graph $\overrightarrow{\Gamma}_K$ is compared with the corresponding edge in the root-directed graph. An *indicator function* σ is defined such that $\sigma(i) = 1$ if $e_i \in \mathcal{G}_0$ has the same direction in $\overrightarrow{\mathcal{G}}_0$ and in $\overrightarrow{\Gamma}_K$, $\sigma(i) = -1$ if they have opposite directions, and $\sigma(i) = 0$ if $e_i \in \mathcal{H}$. Also, the short hand notation σ_i is used for brevity. This function σ returns the values of the path matrix associated to the graph.[51]

Example 1 (cont.): A choice for the directed kinematic graph of the 3URU is shown in Fig. 8a and for the root-directed spanning tree in Fig. 8b. For such a fully parallel manipulator, it is again obvious to introduce the same orientations for the three kinematic chains from ground (v_0) to platform (v_7). Here, $\sigma(i) = 1$ for all $e_i \in \mathcal{G}_0$.

https://doi.org/10.1017/S0263574718000619 Published online by Cambridge University Press

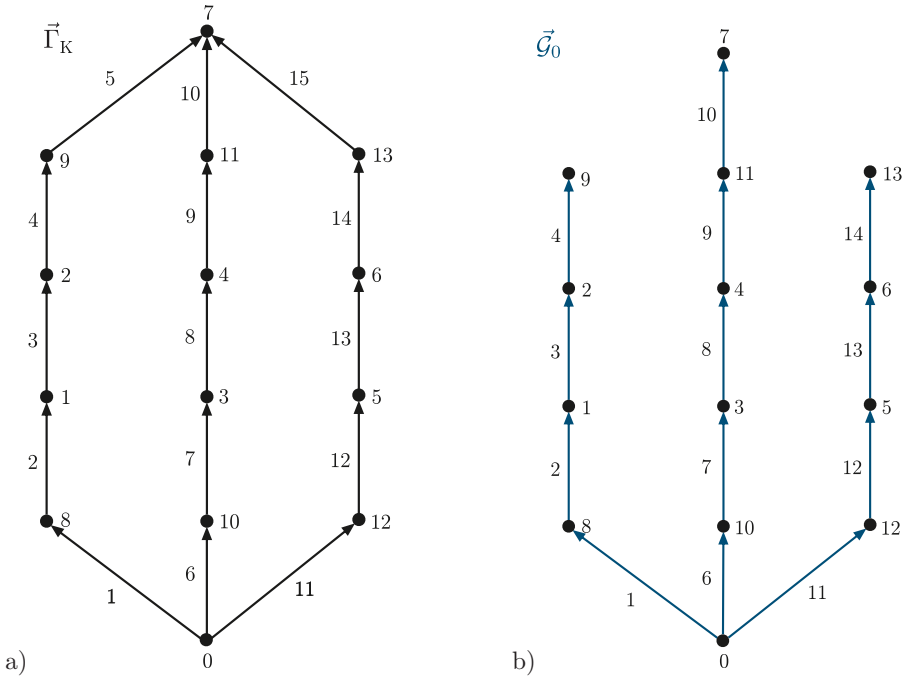


Fig. 8. (a) Directed kinematic graph $\overrightarrow{\Gamma}_K$. Directions indicate the "polarities" of joint variables. (b) Root-directed spanning tree $\vec{\mathcal{G}}_0$ for the 3URU.

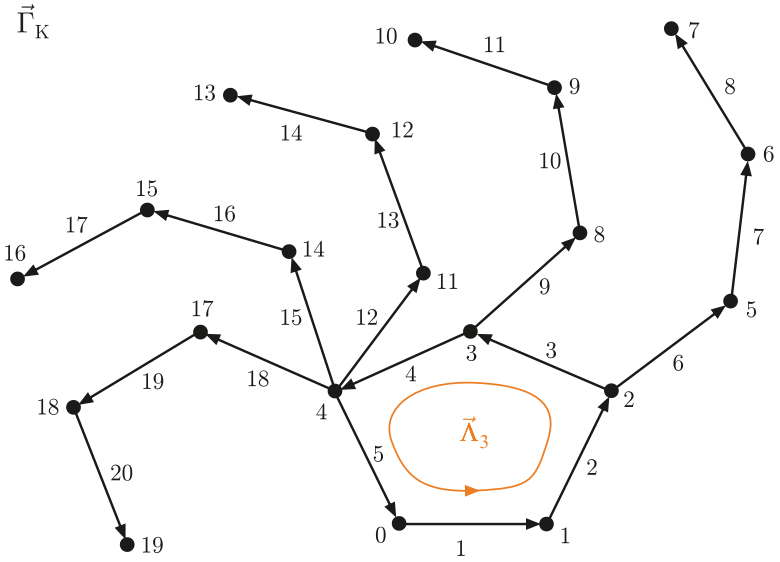


Fig. 9. Directed kinematic graph $\vec{\Gamma}$ and oriented FC $\vec{\Lambda}_3$ for the metamorphic hand.

Example 2 (cont.): For the metamorphic hand, a directed kinematic graph is shown in Fig. 9 and the root-directed spanning tree in Fig. 10. The indicator function is $\sigma(4) = \sigma(5) = -1$ and $\sigma(i) = 1$ otherwise.

Remark 4. For MBS modeling some authors avoid the introduction of the directed kinematic graph and simply adopt the directions from the root-directed spanning tree $\overrightarrow{\mathcal{G}}_0$ in order to define joint orientations.[14,52] Then the orientations of co-tree edges are not specified since in MBS-modeling co-tree joints (cut-joints) are removed and replaced by cut-joint constraints.[25]

https://doi.org/10.1017/S0263574718000619 Published online by Cambridge University Press

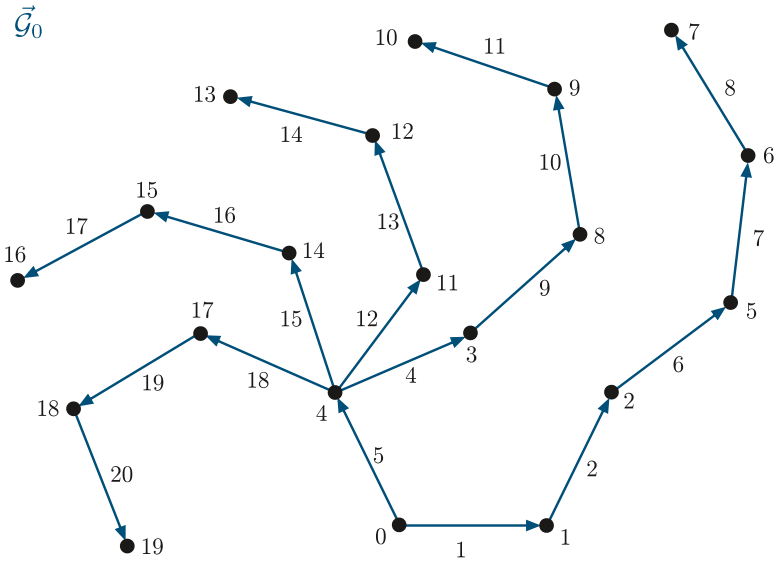


Fig. 10. Root-directed spanning tree $\vec{\mathcal{G}}_0$ for the metamorphic hand.

3.6. Orientation of fundamental cycles

With the direction of a vertex, reflecting the direction of the associated relative motion, it is necessary to indicate the direction in which it is visited when traversing through a FC. To this end, an orientation of the FC Λ_l is introduced such that it coincides with the orientation of its co-tree edge e_l according to the directed kinematic graph. The oriented FC is denoted with $\vec{\Lambda}_l$.

An *indicator function* σ_l is defined on the FC Λ_l such that $\sigma_l(i) = 1$ if e_i has the same direction in $\overrightarrow{\Lambda}_l$ as it has in $\overrightarrow{\Gamma}_{\mathrm{K}}$, $\sigma_l(i) = -1$ if they have opposite directions, and $\sigma_l(i) = 0$ if $e_i \notin \vec{\Lambda}$. Since the orientation of the FC is defined by the co-tree edge e_l it is $\sigma_l(l) = 1$. The short notation $\sigma_{l,i} = \sigma_l(i)$ will be used for sake of compactness. The function σ_l returns the values of circuit matrix of the graph.[51]

Example 1 (cont.): Figure 11a shows the oriented FCs for the 3URU manipulator according to $\mathcal{H}$ in Fig. 6b and $\overrightarrow{\Gamma}_{\mathrm{K}}$ in Fig. 8a. The values of the indicator function are shown in Fig. 11b.

Example 2 (cont.): The metamorphic hand possesses one FC Λ_3. This FC is orientated according to the orientation of $\vec{v}_3 \in \overrightarrow{\Gamma}_{\mathrm{K}}$ (Fig. 9). According to $\overrightarrow{\Gamma}_{\mathrm{K}}$ all edges in Λ_3 have the same directions as the FC. The non-zero values of σ_3 are thus $\sigma_3(i) = 1, i = 1, \ldots, 5$.

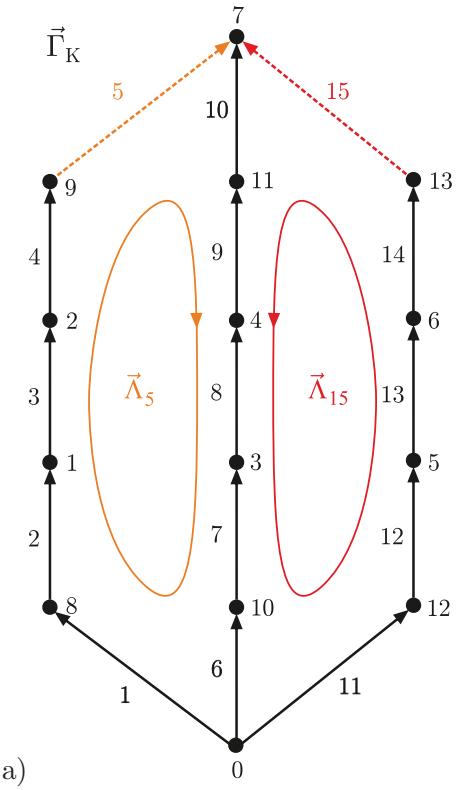
3.7. Ordering on fundamental cycles

The FC Λ_l can be regarded as a closed path that terminates with the edge e_l and starts with the unique edge that has a common vertex with e_l. The latter is referred to as the *starting edge* of the FC Λ_l. The index of this starting edge is denoted with $\bar{l}$.

The orientation of the FC gives rise to a linear ordering on Λ_l and allows for assigning a direct predecessor. Edge e_j is the *direct predecessor* of e_i if e_i comes immediately after e_j when traversing the directed FC $\vec{\Lambda}_l$ starting from e_j to e_l. This is denoted by $e_j = e_i -_l 1$, or simply $j = i -_l 1$. e_j is the pre-predecessor of e_i iff $e_j = (e_i - 1) - 1$. Being its kth predecessor is denoted by $e_j = e_i -_l k$, or simply $j = i -_l k$. Edge e_j is a *predecessor* of e_i iff e_i is in the directed path in $\vec{\Lambda}_l$ from e_j to the terminal e_l. This is denoted by $e_j <_l e_i$, or simply $j <_l i$. Obviously, $e_i \leq e_l$ for all $e_i \in \Lambda_l$. The subscript l is omitted when it is clear that the index arithmetic refers to the FC.

Example 1 (cont.): The FC Λ_5 of the 3URU manipulator in Fig. 11a, for instance, is considered as kinematic chain starting with $\bar{l} = 10$ and terminating wit $l = 5$. According to its orientation it is $e_8 = e_7 - 1$, $e_6 = e_1 - 1$, and $e_i \leq e_5$ for all $e_i \in \Lambda_5$.

https://doi.org/10.1017/S0263574718000619 Published online by Cambridge University Press



a)

b)

i	$\sigma_5(i)$
1	1
2	1
3	1
4	1
5	1
6	-1
7	-1
8	-1
9	-1
10	-1

i	$\sigma_{15}(i)$
6	-1
7	-1
8	-1
9	-1
10	-1
11	1
12	1
13	1
14	1
15	1

Fig. 11. (a) Directed FCs $\vec{\Lambda}_l$ for the 3URU. (b) Indicator functions σ_l for the two FCs. Not listed are the values for edges not in the FCs.

Example 2 (cont.): With the FC Λ_3 oriented according to $\vec{e}_3$ in Fig. 9, it is $\bar{l} = 4$ and $e_4 = e_3 - 1$, $e_1 = e_5 - 1$, for example, and $e_i \leq e_3$ for all $e_i \in \Lambda_3$.

4. Loop Closure Constraints of Linkages in Terms of Joint Screws

4.1. Geometric loop closure constraints

A kinematic loop is a closed kinematic chain. The loop closure gives rise to a system of loop constraints. Different kinematic loops can be identified for a given mechanism in general. A sufficient (but not unique) set of γ kinematic loops is given by the FCs of the kinematic graph, respectively the topological graph.

With assumption 3.1, the edge $e_i \in \Gamma_K$ represents a 1-DOF relative screw motion of adjacent bodies. That is, the kinematic model consists of $n = |E|$ screw joints. Denote with q_i the joint variable associated to $e_i \in \Gamma_K$, and with $\mathbf{q} = (q_1, \ldots, q_n) \in \mathbb{V}^n$ the vector of joint variables of the mechanism. The parameter manifold is $\mathbb{V}^n = \mathbb{T}^{n_R} \times \mathbb{R}^{n_P}$, where n_R is the number of revolute joints and n_P the number of prismatic and screw joints.

A zero reference configuration of the linkage is chosen to which $\mathbf{q} = \mathbf{0}$ is assigned. In this reference configuration the screw coordinate vector (see appendix)

$$\mathbf{Y}_i = \begin{pmatrix} \mathbf{e}_i \\ \mathbf{y}_i \times \mathbf{e}_i + h_i \mathbf{e}_i \end{pmatrix} \in \mathbb{R}^6, \tag{1}$$

is introduced for joint i. Here, $\mathbf{e}_i$ is a unit vector along the joint axis, and $\mathbf{y}_i$ is the position vector of a point on the joint axis, where all vectors are expressed in a global reference frame $\mathcal{F}_0$. The motion relative to the zero reference configuration due to the screw joint can then be expressed as $\exp(\mathbf{Y}_i q_i)$[30,31] with joint variable q_i (see appendix). Concatenating the relative motions of all joints

https://doi.org/10.1017/S0263574718000619 Published online by Cambridge University Press

in the kinematic loop corresponding to the FC Λ_l gives rise to the *geometric loop closure constraints*

$$g_l(\mathbf{q}) = \mathbf{I}, \tag{2}$$

where the *constraint mapping* $g_l : \mathbb{V}^n \to SE(3)$ is

$$g_l(\mathbf{q}) := \exp(\sigma_{l,\bar{l}} q_{\bar{l}} \mathbf{Y}_{\bar{l}}) \cdots \exp(\sigma_{l,l-2} q_{l-2} \mathbf{Y}_{l-2}) \exp(\sigma_{l,l-1} q_{l-1} \mathbf{Y}_{l-1}) \exp(\mathbf{Y}_l q_l), \tag{3}$$

with the index arithmetic understood on the FC (omitting the subscript l).

The expression (2) has been originally introduced by Brockett[3] and since then it is called the "product of exponentials." It provides a simple and compact yet powerful tool for describing the finite motion of a kinematic chain by means of joint screw coordinates $\mathbf{Y}_i$ and joint variables q_i using a single reference frame.

The overall system of geometric constraints $g_l(\mathbf{q}) = \mathbf{I},\ l = 1, \ldots, \gamma$ defines the configuration space (c-space) of the mechanism as the analytic variety

$$\begin{aligned} V &:= g_1^{-1}(\mathbf{I}) \cap \ldots \cap g_\gamma^{-1}(\mathbf{I}) \cap \mathbb{V}^n \\ &= \{\mathbf{q} \in \mathbb{V}^n | g_l(\mathbf{q}) = \mathbf{I},\ l = 1, \ldots, \gamma\}. \end{aligned} \tag{4}$$

Notice that the FCs and hence the loop closure constraints are not unique in general, but the c-space is unique indeed.

Remark 5. The c-space is the central object for mechanism analysis. Its local dimension is by definition equal to the finite local DOF of the mechanism in a given configuration $\mathbf{q} \in V$. Its local geometry further reveals the local mobility in a given configuration $\mathbf{q} \in V$. Since an explicit global description of V, i.e., a solution of the geometric constraints, is not available in general, this has been addressed via the higher order local analysis of V.[4,5,17,21,26,33] This requires the velocity constraints and its time derivatives presented in the next section. The presented systematic formulation is crucial for multi-loop linkages.

Example 1 (cont.): Figure 1 shows the zero reference configuration of the 3URU to which $\mathbf{q} = \mathbf{0}$ is assigned. The global reference frame $\mathcal{F}_0$ is located so to coincide with the platform center when in the reference configuration. Its location is arbitrary, and this particular location is only used because it simplifies the expressions. With the geometry indicated in Fig. 1, and setting $R = a/2$, the joint screw coordinates are

$$\begin{aligned} &\mathbf{Y}_1 = \mathbf{Y}_5 = (-1/2, -\sqrt{3}/2, 0, 0, 0, 0)^T, \mathbf{Y}_2 = (0, 0, 1, -5\sqrt{3}a/4, 5a/4, 0)^T, \\ &\mathbf{Y}_3 = (0, 0, 1, -(1/2 + 3\sqrt{3}/4)a, (3/4 - \sqrt{3}/2)a, 0)^T, \mathbf{Y}_4 = (0, 0, 1, -\sqrt{3}a/4, a/4, 0)^T, \\ &\mathbf{Y}_6 = \mathbf{Y}_{10} = (1, 0, 0, 0, 0, 0)^T, \mathbf{Y}_7 = (0, 0, 1, 0, -5a/2, 0)^T, \\ &\mathbf{Y}_8 = (0, 0, 1, a, -3a/2, 0)^T, \mathbf{Y}_9 = (0, 0, 1, 0, -a/2, 0)^T, \\ &\mathbf{Y}_{10} = \mathbf{Y}_{15} = (-1/2, \sqrt{3}/2, 0, 0, 0, 0)^T, \mathbf{Y}_{12} = (0, 0, 1, 5\sqrt{3}a/4, 5a/4, 0)^T, \\ &\mathbf{Y}_{13} = (0, 0, 1, (3\sqrt{3}/4 - 1/2)a, (3/4 + \sqrt{3}/2)a, 0)^T, \mathbf{Y}_{14} = (0, 0, 1, \sqrt{3}a/4, a/4, 0)^T, \end{aligned} \tag{5}$$

Now consider the FC Λ_5 for instance. The starting vertex of Λ_5 is $\bar{l} = 10$ (Fig. 11) so that the FC can be regarded as a kinematic chain formed by the screw joints $10, \ldots, 6, 1, \ldots, 5$. The orientation of these joints when traversing the FC from 10 to 5 is indicated by the indicator function in Fig. 11b. The constraint mapping for Λ_5 is thus

$$\begin{aligned} g_5(\mathbf{q}) = &\exp(-q_{10}\mathbf{Y}_{10}) \exp(-q_9\mathbf{Y}_9) \exp(-q_8\mathbf{Y}_8) \exp(-q_7\mathbf{Y}_7) \exp(-q_6\mathbf{Y}_6) \\ &\cdot \exp(q_1\mathbf{Y}_1) \exp(q_2\mathbf{Y}_2) \exp(q_3\mathbf{Y}_3) \exp(q_4\mathbf{Y}_4) \exp(q_5\mathbf{Y}_5). \end{aligned}$$

It may be instructive to interpret the vertices of Γ_K that where introduced during the transition from Γ as (auxiliary) rigid bodies. The universal joints of the 3URU shown in Fig. 1 are good examples.

https://doi.org/10.1017/S0263574718000619 Published online by Cambridge University Press

For example, joint 1 is represented by the screw joints corresponding to edges e_1, e_2 and vertex v_8 of Γ_K.

Example 2 (cont.): The metamorphic hand comprises one FC Λ_3 formed by the joints $1, \ldots, 5$, and $\bar{l} = 4$ (Fig. 9). Since $\sigma_3(i) = 1$ for all $e_i \in \Lambda_3$ the constraint mapping is

$$g_3(\mathbf{q}) = \exp(q_4\mathbf{Y}_4)\exp(q_5\mathbf{Y}_5)\exp(q_1\mathbf{Y}_1)\exp(q_2\mathbf{Y}_2)\exp(q_3\mathbf{Y}_3). \tag{6}$$

The screw coordinate vectors are not shown due to space limitation. It should be mentioned, however, that, in order to simplify the resulting expressions for the screw coordinates of the joints in the FC, the global reference frame is located at the spherical center as shown in Fig. 4b. Since the unit vectors $\mathbf{e}_i$ along the axes of joints $i = 1, \ldots, 5$ are parallel to the position vectors $\mathbf{y}_i$ to the respective joint axes (and $h_i = 0$) the translational component in (1) is zero, i.e., $\mathbf{Y}_i = (\mathbf{e}_i, \mathbf{0})^T$, $i = 1, \ldots, 5$. Of course, any other reference frame can be used.

4.2. Velocity constraints

The time derivative of the geometric constraints (2) yields the corresponding velocity constraints for the FC Λ_l. At a configuration $\mathbf{q} \in V$ (i.e., satisfying the geometric constraints) they can be expressed as ref. [27]

$$\sum_{i \in \Lambda_l} \dot{q}_i \mathbf{S}_i^l(\mathbf{q}) = \mathbf{0}. \tag{7}$$

were the instantaneous joint screw coordinate vector of joint i is given by

$$\mathbf{S}_i^l(\mathbf{q}) := \sigma_{l,i}\mathbf{Ad}_{f_{l,i}(\mathbf{q})}\mathbf{Y}_i, \tag{8}$$

with

$$f_{l,i}(\mathbf{q}) := \exp(\sigma_{l,\bar{l}}q_{\bar{l}}\mathbf{Y}_{\bar{l}}) \cdot \ldots \cdot \exp(\sigma_{l,i-2}q_{i-2}\mathbf{Y}_{i-2})\exp(\sigma_{l,i-1}q_{i-1}\mathbf{Y}_{i-1})\exp(\sigma_{l,i}q_i\mathbf{Y}_i). \tag{9}$$

Here $\mathbf{Ad}_{g_{l,i}}$ in (8) is the frame transformation of the screw coordinate vector $\mathbf{Y}_i$ of joint i from the zero reference configuration to the current configuration due to the displacement of joints $\bar{l}, \ldots, i$ in the FC. The index arithmetic in (9) is understood on the FC Λ_l (omitting subscript l).

The velocity constraints are linear in the generalized speeds $\dot{q}_i$, and can hence be expressed using the *geometric constraint Jacobian* $\mathbf{G}_l(\mathbf{q}) : \mathbb{R}^n \to se(3)$ as

$$\mathbf{G}_l(\mathbf{q})\dot{\mathbf{q}} = \mathbf{0}. \tag{10}$$

The non-zero columns of the $6 \times n$ Jacobian $\mathbf{G}_l(\mathbf{q})$ are the "signed" instantaneous screw coordinates $\mathbf{S}_i^l(\mathbf{q})$.

The overall system of velocity constraints for the mechanism is

$$\mathbf{G}(\mathbf{q})\dot{\mathbf{q}} = \mathbf{0}, \tag{11}$$

with the $6\gamma \times n$ constraint Jacobian of the mechanism

$$\mathbf{G}(\mathbf{q}) = \begin{pmatrix} \mathbf{G}_1(\mathbf{q}) \\ \vdots \\ \mathbf{G}_\gamma(\mathbf{q}) \end{pmatrix}. \tag{12}$$

https://doi.org/10.1017/S0263574718000619 Published online by Cambridge University Press

Example 1 (cont.): The constraint Jacobians for the two FCs Λ_5 and Λ_{15} of the 3URU manipulator are readily found to be (omitting dependence on $\mathbf{q}$)

$$\mathbf{G}_5(\mathbf{q}) = \left(\mathbf{S}_1^5,\ \mathbf{S}_2^5,\ \mathbf{S}_3^5,\ \mathbf{S}_4^5,\ \mathbf{S}_5^5,\ \mathbf{S}_6^5,\ \mathbf{S}_7^5,\ \mathbf{S}_8^5,\ \mathbf{S}_9^5,\ \mathbf{S}_{10}^5,\ \mathbf{0},\ \mathbf{0},\ \mathbf{0},\ \mathbf{0},\ \mathbf{0}\right) \in \mathbb{R}^{6,15},$$
$$\mathbf{G}_{15}(\mathbf{q}) = \left(\mathbf{0},\ \mathbf{0},\ \mathbf{0},\ \mathbf{0},\ \mathbf{0},\ \mathbf{S}_6^{15},\ \mathbf{S}_7^{15},\ \mathbf{S}_8^{15},\ \mathbf{S}_9^{15},\ \mathbf{S}_{10}^{15},\ \mathbf{S}_{11}^{15},\ \mathbf{S}_{12}^{15},\ \mathbf{S}_{13}^{15},\ \mathbf{S}_{14}^{15},\ \mathbf{S}_{15}^{15}\right) \in \mathbb{R}^{6,15},$$

where for example $\mathbf{S}_9^5 = -\mathbf{Ad}_{g_{5,9}}\mathbf{Y}_9$, with $g_{5,9}(\mathbf{q}) = \exp(-q_{10}\mathbf{Y}_{10})\exp(-q_9\mathbf{Y}_9)$. Also, with the FC ordering it is $\mathbf{S}_i^5 = \mathbf{S}_i^{15}$ for $i = 6, \ldots, 10$.

Example (cont.): The metamorphic hand possesses one FC Λ_3. The constraint Jacobian for this FC is

$$\mathbf{G}_3(\mathbf{q}) = \left(\mathbf{S}_1^3,\ \mathbf{S}_2^3,\ \mathbf{S}_3^3,\ \mathbf{S}_4^3,\ \mathbf{S}_5^3,\ \mathbf{0},\ \ldots,\ \mathbf{0}\right) \in \mathbb{R}^{6,20}, \tag{13}$$

with $\mathbf{S}_1^3 = \mathbf{Ad}_{f_{3,1}}\mathbf{Y}_1$ and $f_{3,1}(\mathbf{q}) = \exp(q_4\mathbf{Y}_4)\exp(q_5\mathbf{Y}_5)\exp(q_1\mathbf{Y}_1)$, for example.

Remark 6. For local kinematic analysis, the zero reference configuration can always be chosen as the configuration of interest. Then the columns of the constraint Jacobian are simply the reference joint screw coordinate vectors $\sigma_{l,i}\mathbf{Y}_i$ with sign according to the joint polarity within the FC. For example, the constraint Jacobians for the FCs Λ_5 and Λ_{15} of the 3URU are then

$$\mathbf{G}_5(\mathbf{0}) = \left(\mathbf{Y}_1,\ \mathbf{Y}_2,\ \mathbf{Y}_3,\ \mathbf{Y}_4,\ \mathbf{Y}_5,\ -\mathbf{Y}_6,\ -\mathbf{Y}_7,\ -\mathbf{Y}_8,\ -\mathbf{Y}_9,\ -\mathbf{Y}_{10},\ \mathbf{0},\ \mathbf{0},\ \mathbf{0},\ \mathbf{0},\ \mathbf{0}\right)$$
$$\mathbf{G}_{15}(\mathbf{0}) = \left(\mathbf{0},\ \mathbf{0},\ \mathbf{0},\ \mathbf{0},\ \mathbf{0},\ -\mathbf{Y}_6,\ -\mathbf{Y}_7,\ -\mathbf{Y}_8,\ -\mathbf{Y}_9,\ -\mathbf{Y}_{10},\ \mathbf{Y}_{11},\ \mathbf{Y}_{12},\ \mathbf{Y}_{13},\ \mathbf{Y}_{14},\ \mathbf{Y}_{15}\right)$$

The admissible velocities, i.e., the solutions of (11), can be expressed as

$$\dot{\mathbf{q}} = \mathbf{F}\dot{\mathbf{s}}, \tag{14}$$

where $\mathbf{F}$ is an orthogonal complement to the constraint Jacobian $\mathbf{G}$, i.e., $\mathbf{GF} \equiv \mathbf{0}$, and $\dot{\mathbf{s}} = \left(\dot{s}_1, \ldots, \dot{s}_\delta\right)$ are independent generalized velocities. If rank $\mathbf{G}(\mathbf{q}) = r$, then the number of independent generalized coordinates is $\delta(\mathbf{q}) = n - r$. For a mechanism, the joint variables of the actuated joints are usually used as generalized coordinates, presumed that the mechanism is not redundantly actuated[23] and that they are admissible parameters in the considered motion mode. Once the generalized velocities $\dot{\mathbf{s}}$ are selected the joint variables can be rearranged as $\mathbf{q} = (\mathbf{r}, \mathbf{s})$, with the vector of dependent variables $\mathbf{r} = \left(r_1, \ldots, r_r\right)$. The constraint Jacobian can be partitioned accordingly so that (11) becomes

$$\mathbf{G}_1(\mathbf{q})\dot{\mathbf{r}} + \mathbf{G}_2(\mathbf{q})\dot{\mathbf{s}} = \mathbf{0}. \tag{15}$$

Presumed that $\mathbf{G}$ has full rank $r = 6\gamma$, then $\mathbf{G}_1$ is a regular square matrix. An orthogonal complement is then given explicitly as

$$\mathbf{F} = \begin{pmatrix} -\mathbf{G}_1^{-1}\mathbf{G}_2 \\ \mathbf{I}_\delta \end{pmatrix}. \tag{16}$$

For the 3-DOF 3URU manipulator, for example, the three joint angles 1, 6, and 11 can be used as independent coordinates. The 12×15 constraint Jacobian is then partitioned into the corresponding 12×3 submatrix $\mathbf{G}_2$ and the remaining 12×12 matrix $\mathbf{G}_1$. In case of overconstrained mechanisms, or at singular configurations, $\mathbf{G}_1$ is not invertible, which may be handled with a pseudoinverse or screw geometric considerations.

4.3. Acceleration constraints

The time derivative of the velocity constraints yields the acceleration constraints. Crucial for the screw formulation, and the key for compact algebraic expressions, is the relation for the partial derivative

https://doi.org/10.1017/S0263574718000619 Published online by Cambridge University Press

of the instantaneous joint screw coordinate (8). The non-zero terms can be expressed as[24,27]

$$\frac{\partial \mathbf{S}_i^l}{\partial q_j} = [\mathbf{S}_j^l, \mathbf{S}_i^l],\ j <_l i, \tag{17}$$

where the index ordering is understood on the FC Λ_l. Evaluation of the Lie bracket (39) boils down to the evaluation of ordinary cross-products (see appendix). Therewith the acceleration constraints for the FC Λ_l, i.e., the time derivative of (8), are

$$\sum_{i\in\Lambda_l} \left(\ddot{q}_i \mathbf{S}_i^l(\mathbf{q}) + \sum_{j<_l i} \dot{q}_j \dot{q}_i [\mathbf{S}_j^l, \mathbf{S}_i^l] \right) = \mathbf{0}, \tag{18}$$

where the ordering $j <_l i$ is understood on Λ_l.

Example 2 (cont.): The acceleration constraints for the FC Λ_3, for example, are

$$\begin{aligned}
&\ddot{q}_4 \mathbf{S}_4^3 + \\
&\ddot{q}_5 \mathbf{S}_5^3 + \dot{q}_4\dot{q}_5 [\mathbf{S}_4^3, \mathbf{S}_5^3] + \\
&\ddot{q}_1 \mathbf{S}_1^3 + \dot{q}_4\dot{q}_1 [\mathbf{S}_4^3, \mathbf{S}_1^3] + \dot{q}_5\dot{q}_1 [\mathbf{S}_5^3, \mathbf{S}_1^3] + \\
&\ddot{q}_2 \mathbf{S}_2^3 + \dot{q}_4\dot{q}_2 [\mathbf{S}_4^3, \mathbf{S}_2^3] + \dot{q}_5\dot{q}_2 [\mathbf{S}_5^3, \mathbf{S}_2^3] + \dot{q}_1\dot{q}_2 [\mathbf{S}_1^3, \mathbf{S}_2^3] + \\
&\ddot{q}_3 \mathbf{S}_3^3 + \dot{q}_4\dot{q}_3 [\mathbf{S}_4^3, \mathbf{S}_3^3] + \dot{q}_5\dot{q}_3 [\mathbf{S}_5^3, \mathbf{S}_3^3] + \dot{q}_1\dot{q}_3 [\mathbf{S}_1^3, \mathbf{S}_3^3] + \dot{q}_2\dot{q}_3 [\mathbf{S}_2^3, \mathbf{S}_3^3] = \mathbf{0}.
\end{aligned}$$

Remark 7. The relation (17) has important implications for higher order partial derivatives. It was shown[27] that repeated partial derivatives of $\mathbf{S}_i$ w.r.t. the joint variables $q_{\alpha_1}, q_{\alpha_2}, \ldots, q_{\alpha_\nu}$ can be expressed explicitly in terms of nested Lie brackets as

$$\begin{aligned}
\frac{\partial^\nu \mathbf{S}_i^l}{\partial q_{\alpha_1} \partial q_{\alpha_2} \cdots \partial q_{\alpha_\nu}} &= [\mathbf{S}_{\beta_\nu}^l, [\mathbf{S}_{\beta_{\nu-1}}^l, [\mathbf{S}_{\beta_{\nu-2}}^l, \ldots [\mathbf{S}_{\beta_1}^l, \mathbf{S}_i^l] \ldots]]] \\
&= \mathbf{ad}_{\mathbf{S}_{\beta_\nu}^l} \mathbf{ad}_{\mathbf{S}_{\beta_{\nu-1}}^l} \mathbf{ad}_{\mathbf{S}_{\beta_{\nu-2}}^l} \cdots \mathbf{ad}_{\mathbf{S}_{\beta_1}^l} \mathbf{S}_i^l \\
&= \mathbf{ad}_{\mathbf{S}_{\beta_\nu}^l} \frac{\partial^{\nu-1} \mathbf{S}_i^l}{\partial q_{\beta_1} \partial q_{\beta_2} \cdots \partial q_{\beta_{\nu-1}}},
\end{aligned} \tag{19}$$

where $\beta_\nu \leq_l \beta_{\nu-1} \leq_l \cdots \leq_l \beta_1 <_l i$ is the ordered sequence of the indices $\alpha_1, \ldots, \alpha_\nu$. The form (19) allows for explicit algebraic expression of higher order constraints. The latter become complex, however, when written in terms of partial derivatives. This can be avoided by a recursive formulation as presented in ref. [27].

Remark 8. The assumption 3.1 is crucial for the modeling using joint screws, and it is a standard approach to use joint screws in order to define velocity constraints in multi-loop linkages.[2] It allows for modeling of lower pairs and some higher pairs that can be considered as combination of such (e.g., universal joints). For lower pairs, the joint variables are canonical coordinates (exponential coordinates), but it must be noticed that the joint variables only correspond to a local parameterization of joint motions. In case of spherical joints (spatial rotations), the three joint angles are only locally valid due to the well-known parameterization singularities. A valid parameterization can always be introduced for a local kinematic analysis. This is why Davis[8,9] could always assume that there is a system of instantaneous screws that span the twists space of a coupling.

4.4. Summary

The presented formulation of loop closure constraints requires

- The directed kinematic graph $\overrightarrow{\Gamma}_{\mathrm{K}}$.
- A system of oriented FCs $\vec{\Lambda}_l$, $l = 1, \ldots, \gamma$.
- The screw coordinates associated with the 1-DOF joints corresponding to $e_i \in \Gamma_{\mathrm{K}}$.

https://doi.org/10.1017/S0263574718000619 Published online by Cambridge University Press

The modeling can thus start directly with the introduction of the directed kinematic graph and FCs.

5. Forward Kinematics

5.1. Rigid body configurations and end-effector mapping

The rigid body α is represented in the topological graph and in the kinematic graph by its associated vertex $v_\alpha \in \Gamma_K$. There is a unique path in $\mathcal{G}_0$ from v_α to the ground vertex v_0. A body-fixed reference frame is attached to the body. The configuration of body α w.r.t. the global inertial frame $\mathcal{F}_0$ is then represented by $\mathbf{C}_\alpha \in SE(3)$ (see appendix). It is given in terms of joint variables by $\mathbf{C}_\alpha = f_\alpha(\mathbf{q})$, with the *forward kinematic mapping*

$$f_\alpha(\mathbf{q}) := \exp(\sigma_r q_r \mathbf{Y}_r) \cdots \exp(\sigma_{j-2} q_{j-2} \mathbf{Y}_{j-2}) \exp(\sigma_{j-1} q_{j-1} \mathbf{Y}_{j-1}) \exp(\mathbf{Y}_j q_j) \mathbf{A}_\alpha, \tag{20}$$

where $\mathbf{A}_\alpha = \mathbf{C}_\alpha(\mathbf{0}) \in \mathrm{SE}(3)$ is the zero reference configuration assigned to $\mathbf{q} = \mathbf{0}$, i.e., the configuration of the body-fixed reference frame when $\mathbf{q}$ is set to zero. The index arithmetic is understood on $\mathcal{G}_0$. In (20), $j = e(\alpha)$ is the index of the edge connecting v_α to its predecessor, and $r = r(\alpha)$ is the index of the root edge of the path from v_α to v_0.

A mechanism interacts with its environment via an EE (there may be more than one). If an EE is attached to link α and represented by the body-fixed frame, then f_α is called the *EE-mapping* assigned to link α. This is also called the *output-mapping*. In this case, the body-fixed reference frame is the EE-frame and $\mathbf{A}_\alpha$ the reference configuration of the EE.

Example 1 (cont.): The EE of the 3URU manipulator is attached to the platform body $\alpha = 7$. The EE-frame is located at the center of the platform. In the reference configuration, shown in Fig. 1, this coincides with the inertial frame $\mathcal{F}_0$ (a choice often made for mechanism analysis). The reference configuration is thus $\mathbf{A}_7 = \mathbf{I}$. According to the root-oriented spanning tree in Fig. 6a the platform body is connected to the ground via joints $6, \ldots, 10$. That is, $e(7) = 10$ and $r(7) = 6$. Further all joints are positively oriented relative to the root-oriented tree (Fig. 8), so that $\sigma_i = 1$. The EE-mapping is thus

$$f_7(\mathbf{q}) = \exp(q_6 \mathbf{Y}_6) \exp(q_7 \mathbf{Y}_7) \exp(q_8 \mathbf{Y}_8) \exp(q_9 \mathbf{Y}_9) \exp(q_{10} \mathbf{Y}_{10}) \mathbf{A}_7.$$

Example 2 (cont.): Various interaction frames are designated at a robotic hand. In particular a frame is defined at each finger tip in order to model grasping. Consider the thumb with terminal body $\alpha = 7$ and the index finger with terminal body $\alpha = 10$. The respective forward kinematic mapping is, with orientations as in Figs. 9 and 10,

$$\begin{aligned} f_7(\mathbf{q}) &= \exp(q_1 \mathbf{Y}_1) \exp(q_2 \mathbf{Y}_2) \exp(q_6 \mathbf{Y}_6) \exp(q_7 \mathbf{Y}_7) \exp(q_8 \mathbf{Y}_8) \mathbf{A}_7, \\ f_{10}(\mathbf{q}) &= \exp(-q_5 \mathbf{Y}_5) \exp(-q_4 \mathbf{Y}_4) \exp(q_9 \mathbf{Y}_9) \exp(q_{10} \mathbf{Y}_{10}) \exp(q_{11} \mathbf{Y}_{11}) \mathbf{A}_{10}. \end{aligned}$$

All fingers are structurally identical. See Section 6 for systematic treatment.

5.2. Twists of links and EE-Jacobian

The twist of a rigid body can be represented in various ways. For mechanism analysis usually the spatial representation[30] is used denoted by $\mathbf{V}^s = (\boldsymbol{\omega}^s, \mathbf{v}^s)^T$. Here, $\boldsymbol{\omega}^s$ is the angular velocity of the body-fixed frame relative to the spatial inertial frame resolved in the inertial frame, and $\mathbf{v}^s$ is the translational velocity of a point attached to the body momentarily traveling through the origin of the inertial frame resolved in the inertial frame.[30] The spatial twist of body α can be expressed as

$$\mathbf{V}^s_\alpha = \sum_{r \le j \le i} \mathbf{S}_i(\mathbf{q}) \dot{q}_i, \tag{21}$$

with the instantaneous screw coordinates of joint i as part of of the kinematic tree

$$\mathbf{S}_i(\mathbf{q}) := \sigma_i \mathbf{Ad}_{h_i(\mathbf{q})} \mathbf{Y}_i, \tag{22}$$

https://doi.org/10.1017/S0263574718000619 Published online by Cambridge University Press

determined by the frame transformation

$$h_i(\mathbf{q}) := \exp(\sigma_r q_r \mathbf{Y}_r) \cdot \ldots \cdot \exp(\sigma_{i-2} q_{i-2} \mathbf{Y}_{i-2}) \exp(\sigma_{i-1} q_{i-1} \mathbf{Y}_{i-1}) \exp(\sigma_i q_i \mathbf{Y}_i). \tag{23}$$

The ordering and index arithmetic are understood on the spanning tree $\mathcal{G}_0$.

The relation (21) can be summarized as

$$\mathbf{V}^{\mathrm{s}}_{\alpha} = \mathbf{J}^{\mathrm{s}}_{\alpha}(\mathbf{q})\, \dot{\mathbf{q}}, \tag{24}$$

where $\mathbf{J}^{\mathrm{s}}_{\alpha}$ is the *spatial Jacobian* of body α. The non-zero columns of $\mathbf{J}^{\mathrm{s}}_{\alpha}$ are the joint screw coordinate vectors (22). If body α carries an EE, then $\mathbf{J}^{\mathrm{s}}_{\alpha}$ is called the *spatial EE-Jacobian* (or output Jacobian).

For an admissible state $(\mathbf{q}, \dot{\mathbf{q}}) \in T_{\mathbf{q}}V$, i.e., satisfying the geometric and velocity constraints, the body twists, respectively the EE-twists, are determined by (21) respectively (24). The forward kinematic problem consists in determining the body twist as result of the input velocities. If $\dot{\mathbf{s}}$ is the input (actuator) velocities, then the solution to the *forward kinematics problem* of body α is $\mathbf{V}^{\mathrm{s}}_{\alpha} = \mathbf{J}^{\mathrm{s}}_{\alpha}\mathbf{F}\dot{\mathbf{s}}$ where $\mathbf{J}^{\mathrm{s}}_{\alpha}\mathbf{F}$ serves as the *forward kinematics* Jacobian for body α.

Remark 9. In dynamics and grasp analysis, for example, the body-fixed representation $\mathbf{V}^{\mathrm{b}} = (\omega^{\mathrm{b}}, \mathbf{v}^{\mathrm{b}})^T$ of twist is used. Here, ω^{b} is the angular velocity resolved in the body-fixed frame and $\mathbf{v}^{\mathrm{b}}$ is the translational velocity of the origin of the body-fixed frame resolved in that frame. Body-fixed and spatial representations are related by $\mathbf{V}^{\mathrm{s}}_{\alpha} = \mathbf{Ad}_{\mathbf{C}_\alpha}\mathbf{V}^{\mathrm{b}}_{\alpha}$, and $\mathbf{J}^{\mathrm{b}}_{\alpha} = \mathbf{Ad}^{-1}_{\mathbf{C}_\alpha}\mathbf{J}^{\mathrm{s}}_{\alpha}$ is the *body-fixed Jacobian* of body α.

5.3. Summary

The presented formulation for the forward kinematics requires

- The directed kinematic graph $\overrightarrow{\Gamma}_{\mathrm{K}}$.
- A root-directed kinematic graph $\overrightarrow{\mathcal{G}}_0$.
- The screw coordinates associated with the 1-DOF joints corresponding to $e_i \in \mathcal{G}_0$.

6. Modularity

Many mechanisms comprise subsystems that have an identical kinematic setup (but possibly different geometry). The kinematic model can be constructed efficiently by reusing the model of one submodule. A subsystem modeling approach can be introduced formally and systematically making use of the graph representation. Due to the space limitation this cannot be presented here, and only two examples are described.

6.1. Fully parallel manipulators: 3RUR manipulator

Fully parallel manipulators, are characterized by the existence of kinematically identical submodules, for which the 3URU in Fig. 12a is a good example. That is, the kinematic (and topological) graph consists of several identical subgraphs connecting the ground vertex and the platform/EE-vertex. For most PKM the subgraphs are simply a series of vertices, but they can be more complicated subgraphs as for the Delta PKM for instance.

Let the platform body be represented by the vertex $v_\alpha \in \Gamma_{\mathrm{K}}$ and be connected to the ground v_0 by $m = \gamma + 1$ identical kinematic chains. To each of these m chains corresponds a subgraph of Γ_{K}. Denote with $M_s \subset \Gamma_{\mathrm{K}}$ the subgraph corresponding to submodule $s = 1, \ldots, m$. These subgraphs only have the two vertices v_0 and v_α in common. Figure 12b shows the $m = 3$ subgraphs for the 3URU PKM.

One of the m kinematic chains is considered as the *prototypical submodule*. Let this be the chain represented by M_s. The other $m - 1 = \gamma$ submodules can be constructed by relocating the prototypical submodule M_s, i.e., by replacing its reference frame. Further, the joint screw coordinates of the individual submodules can be determined from the joint screw coordinates $\mathbf{Y}_k$, $e_k \in M_s$ of the prototype module via simple frame transformations.

https://doi.org/10.1017/S0263574718000619 Published online by Cambridge University Press

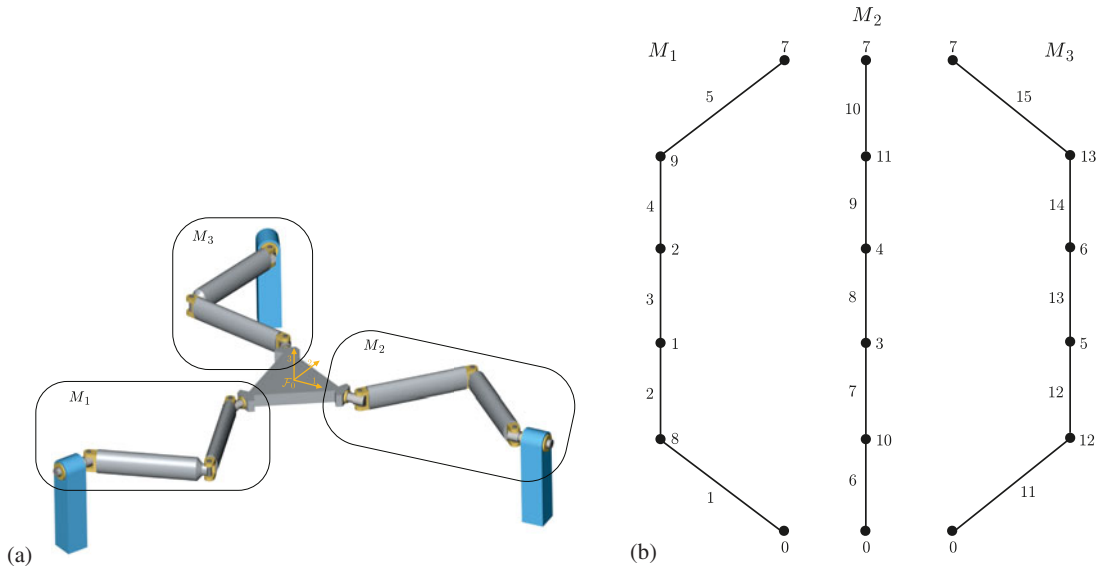


Fig. 12. (a) Submodules of the 3URU manipulator. (b) Subgraphs of Γ_K representing the submodules.

Denote with $\mathbf{M}_{i,s} \in SE(3)$, the transformation necessary to relocate module M_s in order to obtain module M_i. The screw coordinates of M_i are thus

$$\mathbf{Y}_k = \mathbf{Ad}_{\mathbf{M}_{i,s}} \mathbf{Y}_{k'}, e_k \in M_i, e_{k'} \in M_s, \tag{25}$$

where the correspondence of indices k and k' is understood implicitly. For the 3URU, the submodule represented by M_2 in Fig. 12a is taken as the prototype. The screw coordinates in (5) for joints $6, \ldots, 10$ in M_2 are deduced from the inertial frame $\mathcal{F}_0$ in Fig. 12b. The submodule M_1 is obtained by simply rotating $\mathcal{F}_0$ by an angle of $-2\pi/3$ about the 3-axis, and M_3 by a rotation by $2\pi/3$. The respective frame transformations are

$$\mathbf{M}_{1,2} = \begin{pmatrix} -1/2 & \sqrt{3}/2 & 0 & 0 \\ -\sqrt{3}/2 & -1/2 & 0 & 0 \\ 0 & 0 & 1 & 0 \\ 0 & 0 & 0 & 1 \end{pmatrix}, \; \mathbf{M}_{3,2} = \begin{pmatrix} -1/2 & -\sqrt{3}/2 & 0 & 0 \\ \sqrt{3}/2 & -1/2 & 0 & 0 \\ 0 & 0 & 1 & 0 \\ 0 & 0 & 0 & 1 \end{pmatrix}.$$

Indeed, it is readily checked that $\mathbf{Y}_3 = \mathbf{Ad}_{\mathbf{M}_{1,2}} \mathbf{Y}_8$ and $\mathbf{Y}_{13} = \mathbf{Ad}_{\mathbf{M}_{3,2}} \mathbf{Y}_8$ in (5), for example.

6.2. Identical open kinematic chains: Robotic hand

Robotic hands are good examples for mechanisms that are built by combining identical kinematic chains. The metamorphic hand example in Fig. 4 comprises five three-segment fingers with different geometries but identical kinematics. Each finger corresponds to a branch in the kinematic graph. Finger tips are represented by terminal vertices (leave nodes).

Consider a prototypical finger with terminal body α as in Fig. 13a. Its kinematics can be described w.r.t. to the shown reference frame $\mathcal{F}'_\alpha$. Denote with $\mathbf{Y}'_i$ the screw coordinates of its three revolute joints represented in this frame. As in (20) the forward kinematics mapping of the finger w.r.t. to the modeling frame $\mathcal{F}'_\alpha$ is $f'_\alpha(\mathbf{q}) = \exp(\sigma_r q_r \mathbf{Y}'_r) \cdots \exp(\sigma_{j-1} q_{j-1} \mathbf{Y}'_{j-1}) \exp(\mathbf{Y}'_j q_j) \mathbf{A}'_\alpha$. Now, $\mathbf{A}'_\alpha$ is the zero reference configuration relative to $\mathcal{F}'_\alpha$.

The hand kinematics is modeled by attaching a finger model at each of the five mount frames in Fig. 13b.

Let $\mathbf{M}_\alpha \in SE(3)$ be the transformation from the modeling frame $\mathcal{F}'_\alpha$ to the inertial frame $\mathcal{F}_0$. Then the screw coordinates of the joints of the finger with tip vertex α are

$$\mathbf{Y}_i = \mathbf{Ad}_{\mathbf{M}_\alpha} \mathbf{Y}'_i. \tag{26}$$

https://doi.org/10.1017/S0263574718000619 Published online by Cambridge University Press

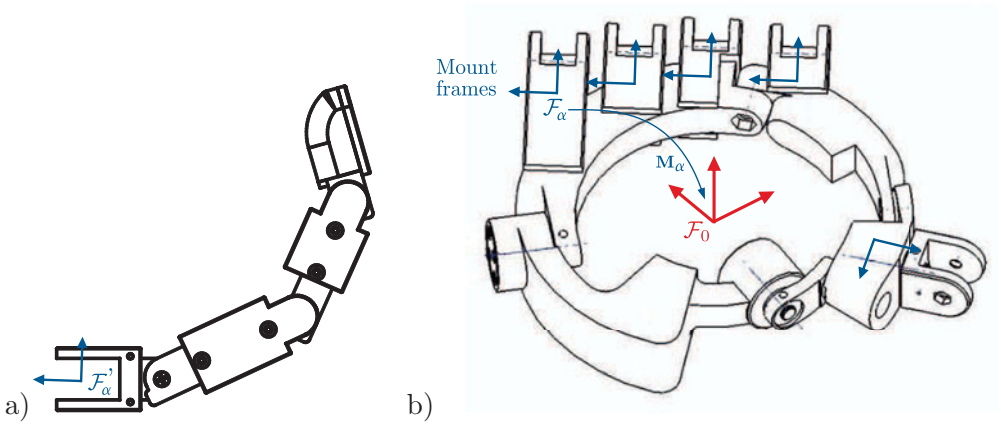


Fig. 13. (a) Single finger with construction frame. (b) Mount frames for fingers at the palm. Figures by courtesy of Guowu Wei and Jian Dai.

The forward kinematics mapping of this finger is then given by (20) with $\mathbf{A}'_\alpha = \mathbf{M}_\alpha \mathbf{A}_\alpha$, that is

$$f_\alpha(\mathbf{q}) = \mathbf{M}_\alpha f'(\mathbf{q}). \tag{27}$$

The forward kinematics Jacobian in (24) is $\mathbf{J}^{\mathrm{s}}_\alpha = \mathbf{Ad}_{\mathbf{M}_\alpha} \mathbf{J}'^{\mathrm{s}}_\alpha$ where $\mathbf{J}'^{\mathrm{s}}_\alpha$ is the forward kinematics Jacobian w.r.t. $\mathcal{F}'_\alpha$. The geometric parameters are specified separately for each finger.

7. Interlude: Motion Spaces, Loop Algebras, and Mobility

A fundamental task in designing a mechanism is to estimate its finite DOF. The determination of the DOF of mechanism with a particular geometry is a difficult task, however. Structural mobility criteria, on the other hand, are considered as simple means to estimate the global DOF from the number and type of joints assuming a generic geometry. Best known is the Chebyshev-Kutzbach-Grübler (CKG) formula.[1,12] With the topological graph representation this can be stated as

$$\delta_{\mathrm{str}} = g(n_B - 1) - \sum_{i=1}^{n_J} (g - \delta_i) \tag{28}$$

$$= g(|B| - 1) - \sum_{i=1}^{|J|} (g - \delta_i) = \sum_{i=1}^{|J|} \delta_i - g\gamma \tag{29}$$

$$= g(|V| - 1) - \sum_{i=1}^{|E|} (g - 1) = n - g\gamma \tag{30}$$

where $\delta_i = \delta(J_i)$ denotes the DOF of joint i (i.e., weight of edge $J_i \in \Gamma$), $n_B := |B|$ is the number of bodies (including the ground), $n := |E|$ is the number of edges of Γ_{K}, and $\gamma = |J| - |B| + 1 = |E| - |V| + 1$ is the number of FC of Γ, respectively, of Γ_{K}. The integer g is the DOF that each body would possess when disconnected from the mechanism, also referred to as the dimension of the "motion space" associated to the mechanism. Common choices are $g = 3$ for planar and spherical, and $g = 6$ for spatial mechanisms. The form (28) is the classical CKG formula that estimates the structural DOF solely from the number of bodies and the DOF of the joints. It simplifies to (30) when assuming 1-DOF joints.

Unfortunately, even for generic geometries, the CKG formula does neither provide a lower nor an upper bound on the finite global DOF. In order to indicate this fact, the result of the CKG is called the structural DOF, denoted by δ_{str}. The problem can be alleviated by taking into account the kinematic topology.

https://doi.org/10.1017/S0263574718000619 Published online by Cambridge University Press

One reason why the CKG formula fails is that it assumes the same dimension g for all bodies. Moreover, g can be interpreted separately for the individual FCs. The term $g\gamma$ in (29), respectively (30), is the total number of (possibly redundant) constraints the n joint variables are subjected to assuming that each FC contributes g constraints. For example, a planar kinematic loop is assumed to impose $g = 3$ and a spatial loop $g = 6$ closure constraints. The assumption that all FCs impose the same number of constraints is not valid, however. Allowing for a different number g_l of constraints for each FC Λ_l, the expressions (29) and (30) yield

$$\delta_{\text{str}} = \sum_{i=1}^{|J|} \delta_i - \sum_{l=1}^{\gamma} g_l = n - \sum_{l=1}^{\gamma} g_l. \tag{31}$$

This amended CKG formula takes into account the different motion characteristics of the FCs. It remains to determine g_l. The closure condition for the FC is that the relative motion, that the kinematic chain allows for when opened, is constrained. Thus the number g_l of constraints is the dimension of the relative motion of the members of the kinematic chain. The number of instantaneous motions of the chain (when cut open) at arbitrary $\mathbf{q} \in \mathbb{V}^n$ is $\dim \mathbf{G}_l(\mathbf{q})$, or in other words, the dimension of the vector space

$$D^l_{\mathbf{q}} := \text{im } \mathbf{G}_l(\mathbf{q}). \tag{32}$$

The vector space that covers the instantaneous motions at any pose $\mathbf{q} \in \mathbb{V}^n$ of the open chain is given by the involutive closure of the distribution D^l, denoted with $\overline{D}^l$. It can be shown that this is given explicitly by

$$\overline{D}^l = \text{span } (\mathbf{Y}_j, \left[\mathbf{Y}_j, \mathbf{Y}_k\right], \left[\mathbf{Y}_j, [\mathbf{Y}_k, \mathbf{Y}_r]\right], j, k, r = \bar{l}, \ldots, l). \tag{33}$$

This is the smallest Lie subalgebra that contains all possible velocities of the open chain. The corresponding Lie subgroup is the smallest SE(3) subgroup containing the possible configurations of all members of the open chain. This leads to

$$g_l := \min(\dim \overline{D}^l, |\Lambda_l|), \tag{34}$$

where $|\Lambda_l|$ is the number of joints in the FC. The form (31) respects the different motion characteristics of individual loops but it cannot overcome the fundamental problems of structural mobility criteria. In particular, g_l is an upper bound on the actual number of independent loop closure constraints for the FC Λ_l, hence the number of independent loop constraints may be smaller even for generic geometries. Further, the FCs are not unique, and different FCs may lead to different g_l. Another fundamental problem of structural mobility criteria is that the interdependence of the constraints imposed by joints is not reflected. This is partly alleviated by (31) but still the structural DOFs of the γ FCs are merely added as if they were disconnected. One way to overcome these limitations and to determine the DOF of mechanisms with generic geometry is to apply combinatorial algorithms operating on the topological graph or constraint graph.[20,39,41–43]

Finally, it must be mentioned that Herve[15,16] has classified linkages upon the loop algebras $\overline{D}^l$, and corresponding motion group, as trivial, exceptional, and paradoxical. Also Rico[34–36] introduced an approach for mobility determination based on these motion groups.

8. Conclusion

The analytic treatment of complex multi-loop linkages requires a systematic formulation of loop closure constraints. It is well known that the kinematics of linkages, i.e., mechanisms comprising lower pair joints, can be modeled in terms of joint screws and the product of exponentials. This applies regardless of the kinematic linkage topology, but in case of multi-loop linkages it requires appropriate definition of independent loops and accordingly an ordering of joints and links. In this paper, an approach was introduced that formalizes the graph representation of linkage topology along with the Lie group and screw formulation of the loop constraints. Both have been scattered over the literature.

https://doi.org/10.1017/S0263574718000619 Published online by Cambridge University Press

Closed from expressions are presented for constraints of arbitrary order (velocity, acceleration, jerk, etc.). The proposed method provides the basis for the kinematic analysis of general linkages. It is briefly discussed how the graph representation can be exploited for modeling modular linkages, i.e., linkages that consists of structurally identical submechanisms (modules).

Acknowledgment
This work has been supported by the "LCM-K2 Center for Symbiotic Mechatronics" within the framework of the Austrian COMET-K2 program.

References

1. R. Alizade, C. Bayram and E. Gezgin, "Structural synthesis of serial platform manipulators," *Mech. Mach. Theory* **42**, 580–599 (2007).
2. D. Basu and A. Ghosal, "Singularity analysis of platform-type multi-loop spatial mechanisms," *Mech. Mach. Theory* **32**(3), 375–389 (1997).
3. R. W. Brockett, "Robotic Manipulators and the Product of Exponentials Formula," *Mathematical Theory of Networks and Systems*, Lecture Notes in Control and Information Sciences, Vol. 58, pp 120–129 (1984).
4. I. F. de Bustos, *et al.*, "Second order mobility analysis of mechanisms using closure equations," **In**: *Meccanica* **47**(7), 1695–1704 (Springer, The Netherlands, 2012).
5. C. Chen, "The order of local mobility of mechanisms," *Mech. Mach. Theory* **46**, 1251–1264 (2011).
6. J. K. Davidson and K. H. Hunt, *Robots and Screw Theory: Applications of Kinematics and Statics to Robotics* (Oxford University Press, Oxford, 2004).
7. T. H. Davis, "Mechanical networks – I,II,III," *Mech. Mach. Theory* **18**(2), 95–112 (1983).
8. T. H. Davies, "Kirchhoff's circulation law applied to multi-loop kinematic chains," *Mech. Mach. Theory* **16**(3), 171–183 (1981).
9. T. H. Davis, "A network approach to mechanisms and machines: Some lessons learned," *Mech. Mach. Theory* **89**, 14–27 (2015).
10. H. Ding, J. Zhao and Z. Huang, "Unified structural synthesis of planar simple and multiple joint kinematic chains," *Mech. Mach. Theory* **45**(4), 555–568 (2012).
11. R. Featherstone *Rigid Body Dynamics Algorithms* (Springer Science and Business Media, New York, 2008).
12. G. Gogu, "Mobility of mechanism: A critical review," *Mech. Mach. Theory* **40**, 1068–1097 (2005).
13. G. Gogu, *Structural Synthesis of Parallel Robots – Part 1: Methodology* (Springer, The Netherlands, 2008).
14. A. Jain, "Graph theoretic foundations of multibody dynamics, Part I: Structural properties," *Multibody Syst. Dyn.* **26**, 307–333 (2011).
15. J. M. Hervé, "Analyse structurelle des mécanismes par groupe des déplacements," *Mech. Mach. Theory* **13**, 437–450 (1978).
16. J. M. Hervé, "Intrinsic formulation of problems of geometry and kinematics of mechanisms," *Mech. Mach. Theory* **17**(3), 179–184 (1982).
17. J. Kieffer, "Differential analysis of bifurcations and isolated singularities of robots and mechanisms," *IEEE T. Rob. Automat.* **10**(1), 1–10 (1994).
18. G. Laman, "On graphs and the rigidity of plane skeletal structures," *J. Eng. Math.* **4**, 331–340 (1970).
19. A. Lee and I. Streinu, "Pebble Game Algorithms and (k, l)-Sparse Graphs," *Proceedings of the European Conference on Combinatorics, Graph Theory and Applications (EuroComb '05)* (2005).
20. A. Lee and I. Streinu, "Pebble game algorithms and sparse graphs," *Discrete Math.* **308**(8), 1425–1437 (1425).
21. J. Lerbet, "Analytic geometry and singularities of mechanisms," *ZAMM, Z. Angew. Math. Mech.* **78**(10b), 687–694 (1999).
22. J.-P. Merlet, *Optimal design of robots, Robotics: Science and Systems* (Cambridge, MA, USA, 2005).
23. A. Müller, "On the terminology and geometric aspects of redundantly actuated parallel manipulators," *Robotica* **31**(1), 137–147 (2013).
24. A. Müller, "Higher derivatives of the kinematic mapping and some applications," *Mech. Mach. Theory* **76**, 70–85 (2014).
25. A. Müller, "Representation of the kinematic topology of mechanisms for kinematic analysis," *Mech. Sci.* **6**, 1–10, (2015).
26. A. Müller, "Local kinematic analysis of closed-loop linkages -mobility, Singularities, and Shakiness," *ASME J. Mech. Rob.* **8**, 041013-1 (2016).
27. A. Müller, "Recursive higher-order constraints for linkages with lower kinematic pairs," *Mech. Mach. Theory* **100**, 33–43 (2016).
28. A. Müller, "Coordinate mappings for rigid body motions," *ASME J. Comput. Nonlinear Dyn.* **12**(2), (2016).
29. A. Müller and O. Shai, "Constraint graphs for combinatorial mobility determination," *Mech. Mach. Theory* **108**, 260–275 (2017).
30. R. M. Murray, Z. Li and S. S. Sastry, *A Mathematical Introduction to Robotic Manipulation* (CRC Press, Boca Raton, 1994).

https://doi.org/10.1017/S0263574718000619 Published online by Cambridge University Press

31. F. C. Park and K. M. Lynch, *Modern Robotics: Mechanics, Planning and Control* (Cambridge University Press, Cambridge, 2017).
32. S. R. Ploen and F. C. Park, "Coordinate-invariant algorithms for robot dynamics," *IEEE Tran. Rob. Automat. Soc.* **15**(6), 1130–1135 (1999).
33. J. M. Rico, J. Gallardo and J. Duffy, "Screw theory and higher order kinematic analysis of open serial and closed chains," *Mech. Mach. Theory* **34**(4), 559–586 (1999).
34. J. M. Rico, J. Gallargo and B. Ravani, "Lie algebra and the mobility of kinematic chains," *J. Robot. Syst.* **20**(8), 477–499 (2003).
35. J. M. Rico and B. Ravani, "On mobility analysis of linkages using group theory," *ASME J. Mech. Des.* **125**, 70–80 (2003).
36. J. M. Rico, L. D. Aguilera, J. Gallardo, R. Rodriguez, H. Orozco and J. M. Barrera, "A more general mobility criterion for parallel platforms," *ASME J. Mech. Des.* **128**, 207–219 (2004).
37. N. Rojas and F. Thomas, Forward Kinematics of the General Triple-Arm Robot Using a Distance-Based Formulation, **In**: *Proc. Computational Kinematics* (Said Zeghloul, Lotfi Romdhane and Med Amine Larib, eds.) (Springer International Publishing, Cham, Switzerland, 2017) pp. 257–26.
38. V. Pozhbelko, "A unified structure theory of multibody open-, closed-, and mixed-loop mechanical systems with simple and multiple joint kinematic chains," *Mech. Mach. Theory* **100**, 1–16 (2016).
39. B. Schulze, A. Sljoka and W. Whiteley, "How does symmetry impact the flexibility of proteins," *Philos. Trans. A Math. Phys. Eng. Sci.* **372**, (2014).
40. J. Selig, *Geometric Fundamentals of Robotics* (Monographs in Computer Science Series) (Springer-Verlag, New York, 2005).
41. A. Sljoka, *Algorithms in Rigidity Theory with Applications to Protein Flexibility and Mechanical Linkages* (York University, Toronto, 2012).
42. A. Sljoka, O. Shai and W. Whiteley, "Checking Mobility and Decomposition of Linkages Via Pebble Game Algorithm," *ASME Design Engineering Technical Conferences (IDETC)*, August 28–31 (2011) Washington, USA.
43. O. Shai, A. Sljoka and W. Whiteley, "Directed graphs," *Decompositions, Spatial Rigidity, Discrete Appl. Math.* **161**, 3028–3047 (2013).
44. K. Sugimoto, "Kinematic analysis and derivation of equations of motion for mechanisms with loops of different motion spaces (theoretical analysis)," *JSME Int. J. Series C Mech. Syst., Mach. Elements Manuf.* **44**(3), 610–617 (2001).
45. D. Talabă, "Mechanical models and the mobility of robots and mechanisms," *Robotica* **33**(1), 181–193 (2015).
46. J. J. Uicker, B. Ravani and P. N. Sheth *Matrix Methods in the Design Analysis of Mechanisms and Multibody Systems* (Cambridge University Press, Cambridge, 2013).
47. G. Wei, S. Dai, S. Wang and H. Luo, "Kinematic analysis and prototype of a metamorphic anthropomorphic hand with a reconfigurable palm," *Int. J. Human. Robot.* **08**(3), 459–479 (2011).
48. N. White and W. Whiteley, "The algebraic geometry of motions of bar-and-body frameworks," *SIAM J. Algebr. Discrete Meth.* **8**(1), 1–32 (1987).
49. W. Whiteley, "Counting out to the flexibility of molecules," *Phys. Biol.* **2**, S116–S126 (2005).
50. W. Whiteley, "Rigidity and Scene Analysis," **In**: *Handbook of Discrete and Computational Geometry*, 2nd ed. (J. E. Goodman and J. O'Rourke, eds.) (Chapman and Hall/CRC, 2004).
51. J. Wittenburg, *Dynamics of Systems of Rigid Bodies* B. G. Teubner, Stuttgart (1977).
52. J. Wittenburg, *Dynamics of Multibody Systems* 2nd ed. (Springer-Verlag, Berlin Heidelberg, 2008).
53. K. Wohlhart, "Screw Spaces and Connectivities in Multiloop Linkages," **In**: *On Advances in Robot Kinematics* (J. Lenarčič and C. Galletti, eds.) (Springer, Dordrecht, 2004) pp. 97–104.
54. H.-S. Yan, *Creative Design of Mechanical Devices* (Springer, 1998).
55. D. Zlatanov, I. A. Bonev and C. M. Gosselin, "Constraint Singularities as C-Space Singularities," **In**: *Advances in Robot Kinematics, Theory And Application* (J. Lenarčič and F. Thomas, eds.) (Springer, Dordrecht, 2002) 183–192.

Appendix: Rigid Body Motions and the Lie Group SE (3)

In this section, the basic expressions for the Lie group modeling of rigid body motions and kinematic chains are given that are used in the paper. Details can be found in the text books.[30,31,40] In the following, $\widetilde{\mathbf{x}} \in so(3)$ denotes the scew symmetric matrix associated to the vector $\mathbf{x} \in \mathbb{R}^3$.

A rigid body is kinematically represented by a body-fixed reference frame. The absolute (or global) *configuration* of a rigid body refers to its orientation and translation relative to global inertial frame $\mathcal{F}_0$. The absolute configuration of a body (i.e., of its reference frame) is represented by a rotation matrix $\mathbf{R} \in \mathrm{SO}(3)$ and a position vector $\mathbf{r} \in \mathbb{R}^3$ that are summarized as $C = (\mathbf{R}, \mathbf{r}) \in \mathrm{SE}(3)$. It is customary to represent these frame transformations as 4×4 matrices (also called "homogenous"

https://doi.org/10.1017/S0263574718000619 Published online by Cambridge University Press

transformation matrices)

$$\mathbf{C} = \begin{pmatrix} \mathbf{R} & \mathbf{r} \\ \mathbf{0} & 1 \end{pmatrix} \in \mathrm{SE}(3)\,. \tag{35}$$

Here, $\mathrm{SE}(3) = \mathrm{SO}(3) \ltimes \mathbb{R}^3$ is the Lie group of rigid body motions.[30,31] The concatenation of two frame transformations is described by multiplication $C_1 \cdot C_2 = (\mathbf{R}_1\mathbf{R}_2, \mathbf{r}_1 + \mathbf{R}_1\mathbf{r}_2)$. This is conveniently expressed by the matrix multiplication $\mathbf{C}_1 \cdot \mathbf{C}_2$. In this notation, the 4×4 identity matrix $\mathbf{I}$ is the identity element. Any rigid body motion, i.e., frame transformation, can be achieved by a screw motion, i.e., a rotation about an axis together with a translation along that axis. To the frame transformation that takes a given reference frame $\mathcal{F}$ (rigid body) from its initial configuration to its current can be associated the screw coordinate vector $\mathbf{Y} = (\mathbf{e}, \mathbf{y} \times \mathbf{e} + h\mathbf{e})^T \in \mathbb{R}^6$, where $\mathbf{e} \in \mathbb{R}^3$ is the unit vector along the screw axis and $\mathbf{y} \in \mathbb{R}^3$ the position vector to a point on that axis measured from the origin of the reference frame $\mathcal{F}$. Both vectors are resolved in $\mathcal{F}$. The finite screw motion, i.e., the frame transformation, is then described by the exponential mapping as $\mathbf{C} = \exp(\varphi\mathbf{Y})$ that can be expressed as

$$\begin{aligned} \exp(\varphi\mathbf{Y}) &= \begin{pmatrix} \mathbf{R}(\varphi\mathbf{e}) & (\mathbf{I} - \mathbf{R})\mathbf{p} + \varphi h\mathbf{e} \\ \mathbf{0} & 1 \end{pmatrix}, \text{ for } h \neq \infty \\ &= \begin{pmatrix} \mathbf{I} & \varphi\mathbf{e} \\ \mathbf{0} & 1 \end{pmatrix}, \text{ for } h = \infty \end{aligned} \tag{36}$$

where $\mathbf{R} = \exp(\varphi\mathbf{e})$ is the rotation matrix given by the Euler–Rodrigues formula[28]

$$\exp(\varphi\mathbf{e}) = \mathbf{I} + \sin\varphi\widetilde{\mathbf{e}} + (1 - \cos\varphi)\,\widetilde{\mathbf{e}}^2. \tag{37}$$

For finite pitch $h \in \mathbb{R}$, the variable φ is the rotation angle ($h = 0$ for pure rotation). For pure translations, h is considered to be infinite and φ is the translation variable.

If the screw coordinate vector $\mathbf{Y}$ is associated to a screw joint connecting a rigid body, and expressed in the inertial frame $\mathcal{F}_0$, then $\exp(\varphi\mathbf{Y})$ determines the absolute displacement of the body due to the joint motion.

Screws are geometric entities and hence frame invariant. But screw coordinates are represented in a particular frame $\mathcal{F}$. The transformation of screw coordinates to another frame is achieved by the adjoined mapping. Let $\mathbf{C} \in \mathrm{SE}(3)$ describe the transformation from the frame $\mathcal{F}$ to a new frame $\mathcal{F}'$. The transformation of the screw coordinate vector $\mathbf{Y}$ to the representation in the frame $\mathcal{F}'$ is then $\mathbf{Y}' = \mathbf{Ad}_\mathbf{C}\mathbf{Y}$, where

$$\mathbf{Ad}_\mathbf{C} = \begin{pmatrix} \mathbf{R} & \mathbf{0} \\ \widetilde{\mathbf{r}}\mathbf{R} & \mathbf{R} \end{pmatrix} \tag{38}$$

is the adjoined mapping to $\mathbf{C}$ in (35).

Let $\mathbf{X} = (\boldsymbol{\xi}, \boldsymbol{\eta})^T$ be a general screw coordinate vector. The Lie bracket, respectively, screw product, of two screw coordinate vectors $\mathbf{X}_1$ and $\mathbf{X}_2$ is defined as

$$[\mathbf{X}_1, \mathbf{X}_2] = \left(\boldsymbol{\xi}_1 \times \boldsymbol{\xi}_2, \boldsymbol{\eta}_1 \times \boldsymbol{\xi}_2 + \boldsymbol{\xi}_1 \times \boldsymbol{\eta}_2\right)^T = \mathbf{ad}_{\mathbf{X}_1}\mathbf{X}_2, \tag{39}$$

which can be expressed using the adjoined operator matrix

$$\mathbf{ad}_\mathbf{X} = \begin{pmatrix} \widetilde{\boldsymbol{\xi}} & \mathbf{0} \\ \widetilde{\boldsymbol{\eta}} & \widetilde{\boldsymbol{\xi}} \end{pmatrix}. \tag{40}$$

https://doi.org/10.1017/S0263574718000619 Published online by Cambridge University Press